Preparation and characterization of in-situ graphite powder reinforced titanium-based composites

(In-Situ 黒鉛粉末強化チタン基複合
材料の組織制御及びその特性評価)

WANG NING

April 2024

Preparation and characterization of in-situ graphite powder reinforced titanium-based composites

(In-Situ 黒鉛粉末強化チタン基複合材料
の組織制御及びその特性評価)

Dissertation for the Degree of
Doctor of Philosophy

Mechanical Engineering Program
Graduate School of Engineering
Hiroshima University, Japan

Assoc. Prof. Choi Yong Bum, Advisor
WANG NING

April 2024

CONTENTS

Contents
List of Figures
List of Tables
Chapter 1 Background and objectives
1.1 Introduction 2
1.2 Structure and properties of titanium carbide (TiC) 4
1.3 Synthesis method of TMCs and existing problems at present stage 7
1.3.1 Powder metallurgy (PM) 7
1.3.2 Self-propagating High-temperature Synthesis (SHS) 7
1.3.3 Reaction hot pressing (RHP) 7
1.3.4 Exothermic diffusion method (XDTM) 8
1.3.5 Mechanical alloying (MA) 8
1.3.6 Melting method (MM) 9
1.4 The choice of matrix and reinforcement 9
1.4.1 The choice of matrix 9
1.4.2 The choice of reinforcement 11
1.5 Advantages and prospects of preparing titanium matrix composites by SPS 13
1.6 Problem of previous studies and objectives of this study 16
1.7 Outline of this study 18
References 19

Chapter 2 Fabrication of In-Situ TiC Particles reinforced Ti Matrix Composites with graphite powder sheets
2.1 Introduction 23
2.2 Experimental procedure 25
2.2.1 Raw materials 25

2.2.2 Fabrication of graphite powder sheet *25*

2.2.3 Reaction of single layer of graphite powder sheet and Ti plates *26*

2.3 Results and discussion *27*

2.3.1 Microstructures *27*

2.3.2 TiC reaction rate and mechanism *30*

2.3.3 Diffusion mechanism of titanium carbide *33*

Summary *34*

References *35*

Chapter 3 Fabrication of In-Situ Rod-like TiC Particles Dispersed Ti Matrix Composites

3.1 Introduction *38*

3.2 Experimental procedure *40*

3.2.1 Raw materials *40*

3.2.2 Fabrication of graphite powder sheet *40*

3.2.3 Fabrication of TMCs with multi-layer graphite powder sheets *41*

3.2.4 Hot forging of composite materials *43*

3.3 Results and discussion *44*

3.3.1 XRD *44*

3.3.2 Microstructure *45*

3.3.3 Tensile testing and strengthening mechanism analysis *49*

Summary *53*

References *54*

Chapter 4 Effect of C content on the microstructure and properties of in-situ synthesized TiC particles reinforced Ti composites

4.1 Introduction *56*

4.2 Experimental procedure *58*

4.2.1 Preparation of graphite powder sheets *58*

4.2.2 Fabrication of TiC/Ti composites *58*

4.2.3 Characterization of TiC/Ti composites *59*
4.3 Results and discussions *60*
4.3.2 Microstructure characterization *61*
4.3.3 Tensile testing *64*
4.4 Discussion *67*
4.4.1 Formation and Morphological Evolution of TiC *67*
4.4.2 Strengthening mechanisms. *69*
4.5 Summary *72*
References *73*
Chapter 5 Conclusion
Conclusions *75*

List of Figures

Fig.1.1 The schematic diagram of the ORs of TiC and α-Ti.

Fig. 1.2 Schematic view of SPS.

Fig. 2.1 Composition weight ratio of the civil aviation aircraft

Fig. 2.2. Schematic illustration of fabricating processes of Graphite powder sheet.

Fig. 2.3. SEM images of Ti matrix composite by different of sintering temperature: 873K(a), 973K(b), 1073K(c), 1173K(d) and 1273K (e); (a')-(e'): Corresponding replication view of the residual graphite.

Fig. 2.4. (a) BSE image and area mapping by EPMA of bonding area of TMC of 1073 K; (b) BSE image of TMC of 1273 K; (c) Schematic illustration of synthetic process of in-situ TiC particles dispersed TMC.

Fig. 2.5. FE-SEM image and point analysis by EDS of TiC reinforced TMC sintered at 1273 K.

Fig. 2.6. XRD pattern of TiC reinforced TMC sintered with different sintering temperature.

Fig. 2.7 Image of Arrhenius plot.

Fig. 2.8 Schematic illustration of solid-state reaction mechanisms in Ti and C diffusion-couple.

Fig. 3.1. Schematic illustration of fabricating processes of Graphite powder sheet: (a) the SEM image of graphite powder sheet.

Fig. 3.2 Schematic illustration of processes of spark plasma sintering for large size.

Fig. 3.3. (a) Schematic illustrations of preparation processes of large-scale samples; (b) Image of shape of tensile specimen (ASTM test method E8M-11, unit: mm)

Fig. 3.4. XRD pattern of TiC reinforced TMC sintered with different sintering temperature.

Fig. 3.5. (a) BSE images of TiC reinforced TMCs sintering at 1273K for 0.6 ks; (b) 1473K for 0.6 ks; (c) and (d) 1473K for 3.6 ks; (e) The schematic diagram of the ORs of TiC and α-Ti.

Fig. 3.6 Results of EPMA mapping and SEM image of TiC/Ti composite sintered at 1473K by SPS.

Fig. 3.7. Tensile strength-displacement curve of of pure Ti and TiC reinforced TMC at 1473K for 3.6k s.

Fig. 3.8. (a) SEM images of fracture surface of TiC reinforced TMC at 1473K for 3.6k s; (b) magnified image.

Fig.3.9 (a) OM images of TiC/Ti composite and TiC/Ti composite after hot-forging. (b) Measured values of micro vickers hardness test. (c) Application in golf clubs.

Fig. 4.1. (a) Schematic illustration of fabricating processes of graphite powder sheet; (b) sintering process of TiC/Ti composites; (c) size of plate tensile specimen.

Fig. 4.2. X-ray diffraction pattern of deposited samples with different C content

Fig. 4.3. Distributions of TiC particles inside of the TiC/Ti composites with different C content: (a) 0.18 wt.% of TMC-P; (b) 1.27 wt.% of TMC-1; (c) 1.81 wt.% of TMC-2; (d) 3.91 wt.% of TMC-3; (a') - (d') corresponding magnified mapping images.

Fig. 4.4. Room temperature tensile stress-strain curve of deposited TiC/Ti composites.

Fig. 4.5. Scanning electron micrographs of tensile fracture surface of the titanium matrix composites tested with different C content: (a) 1.27 wt% of TMC-1; (b) 1.81 wt% of TMC-2; (c) 3.91 wt% of TMC-3.

Fig. 4.6. Schematic shown crack propagation mechanisms for two types of structure.

List of Tables

Table.1.1 Properties of TiC at room temperature.

Table 1.2 Physical and mechanical properties of reinforcement

Table 2.1. Properties of pure titanium.

Table 3.1 Conditions of hot forging.

Chapter 1

Background and objectives

1.1 Introduction 2

1.2 Structure and properties of titanium carbide (TiC) 4

1.3 Synthesis method of TMCs and existing problems at present stage 7

1.3.1 Powder metallurgy (PM) 7

1.3.2 Self-propagating High-temperature Synthesis (SHS) 7

1.3.3 Reaction hot pressing (RHP) 7

1.3.4 Exothermic diffusion method (XDTM) 8

1.3.5 Mechanical alloying (MA) 8

1.3.6 Melting method (MM) 9

1.4 The choice of matrix and reinforcement 9

1.4.1 The choice of matrix 9

1.4.2 The choice of reinforcement 11

1.5 Advantages and prospects of preparing titanium matrix composites by SPS 13

1.6 Problem of previous studies and objectives of this study 16

1.7 Outline of this study 18

References 19

1.1 Introduction

Since 1950, titanium and its alloys have been highly respected and have become the focus of research in various fields. These alloys are known for their unique properties, including high strength-to-weight ratio, light weight, corrosion resistance and biocompatibility, and are therefore widely recognized in industries such as biomedical, automotive, petrochemical and aerospace [1]. In addition, titanium matrix composites formed from titanium alloy matrix and fiber, particle or whisker reinforcement have excellent properties such as high modulus, high strength-to-weight ratio, high temperature and wear resistance, as well as the potential for weight reduction. [2]

Over the past 30 years, titanium matrix composites have gradually replaced nickel-based alloys in the aerospace sector, especially in high-performance applications such as rotating components for jet engine compressors [3]. This indicates that titanium matrix composites have high potential and application prospects in the field of aerospace. However, despite their advantages, their widespread application in industry is limited by the complexity of manufacturing composites and the high costs associated with material processing. [4] For instance, the U.S. land combat vehicles replaced steel with titanium alloy components, significantly improving ballistic resistance while reducing the overall vehicle weight by 65%[5]. VW chose to use TC4 (Ti-6Al-4V) alloy as the material for connecting rods in automobiles, effectively reducing engine weight, enhancing fuel efficiency, and lowering emissions [6]. According to the statistics from the Titanium Zirconium Hafnium Sub-association of the China Nonferrous Metals Industry Association, the largest usage of titanium in China is in the chemical industry, accounting for 50%, followed by the aerospace industry. In 2022, titanium usage in the chemical industry was 73,000 tons, representing 50%, while in the aerospace industry, it was

33,000 tons, accounting for 23% [7]. The usage of titanium in the medical and shipbuilding fields is relatively low, but the growth rate exceeds 30%. The characteristics of titanium and titanium alloys include: (1) high strength, with tensile strength ranging from 686 to 1,176 MPa, and a density about 60% that of steel; (2) higher hardness, with the Rockwell hardness (HRC) of titanium alloys after annealing ranging from 32 to 38; (3) excellent performance at high and low temperatures, showing superior mechanical properties compared to traditional materials such as steel and aluminum, especially in terms of heat resistance [8]. As China's industry advances into high-tech fields, the importance of titanium and its alloys in the national economy has grown, with widespread applications in aerospace, marine engineering, chemical industry, and petroleum industry. Due to their high strength-to-weight ratio, corrosion resistance, good low-temperature performance, and significant chemical reactivity, titanium alloys are classified into α, α+β, and β3 categories, and industrial pure titanium is categorized as TA1, TA2, TA3, TA4, and titanium-palladium alloys as TA9, TA10 (titanium-molybdenum-nickel alloy) [5]. As an active metal, titanium exhibits good welding properties under proper cleaning and protection. Early research primarily focused on silicon carbide fiber-reinforced titanium-based composites, which significantly improved the mechanical properties of the matrix alloy. However, these materials were constrained by factors such as high cost, complex processing, anisotropy, and interface reactions [9]. Therefore, non-continuous reinforced titanium-based composites have become a crucial research direction. These materials can be categorized based on the reinforcement generation method into external addition and in-situ synthesis processes. In order to address issues arising from traditional external addition methods, in-situ synthesis technology has been developed to prepare non-continuous reinforced titanium-based composites through chemical reactions among elements in the raw materials.

1.2 Structure and properties of titanium carbide (TiC)

Titanium carbide, denoted by the chemical formula TiC, adopts a cubic crystal system with a NaCl-type structure and belongs to the Fm3m space group (Z = 4). The lattice constant is represented by a = 0.4327 nm. While Ti atoms are positioned at the origin (0,0,0), C atoms are situated at the (1/2,1/2,1/2) positions. The coordination between Ti and C atoms is octahedral, and Ti_6C octahedra share edges. The schematic structure of titanium carbide is depicted in Fig. 1.1, where (a) illustrates the typical crystal arrangement of TiC. In this structure, C atoms occupy octahedral positions, forming a hexagonal shape when viewed along the direction perpendicular to the planes, as shown in (b) [10].

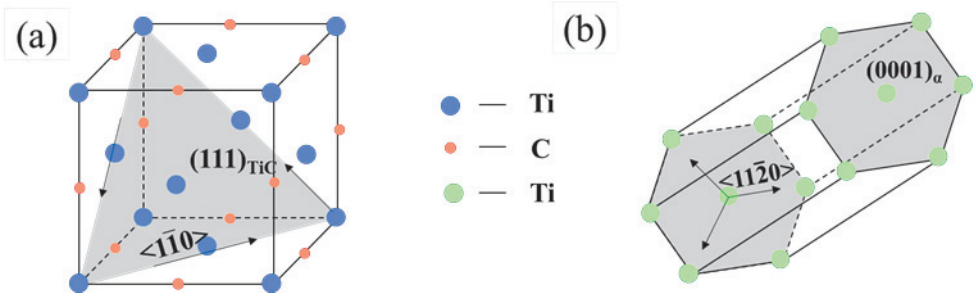

Fig.1.1 The schematic diagram of the ORs of TiC and α-Ti.

The mechanical properties, unique electrical characteristics, and high-temperature strength of titanium carbide particles make them highly effective as a reinforcement phase in composites. Fine-grained TiC contributes to enhancing the yield strength of composites through mechanisms involving dispersion and grain size, and it improves toughness by impeding crack propagation [11]. Table 1 provides a summary of the electrical, mechanical, chemical, and thermal properties of titanium carbide at room temperature.

Table.1 Properties of TiC at room temperature [12].

Electrical properties	
Molecular Weight	59.91
Density ($g.cm^{-3}$)	4.91
Electrical conductivity (10^6 $S.cm^{-1}$)	30
Electrical resistivity (μΩ.cm)	68
Hall constant (10^{-4} $cm^3/A.s$)	-15
Magnetic susceptibility (10^{-6} emu/mol)	-7.5
Superconductive transition temperature (K)	115
Mechanical properties	
Vickers hardness (GPa)	28-35
Young's modulus (GPa)	410-510
Shear modulus (GPa)	186
Flexure strength (MPa)	240-390
Poisson's ratio	0.191
Chemical properties	
Chemical symbol	TiC
Color	Silver gray
Electronic configuration	Ti^{+}_{+}[Ar]$3d^2 4s^2$
	C^{+}_{+}[He]$2s^2 2p^2$
Chemical composition (%)	Ti content (79.95)
	C content (20.05)
Structure	Cubic B1 (NaCl)
Lattice parameter (nm)	0.4328
Space group	*Fm3m*

Pearson symbol	cF8
Thermal properties	
Melting temperature (°C)	3067
Boiling temperature (°C)	4820
Thermal conductivity (°C)	21
Enthalpy of formation ($kJ.mol^{-1}$)	-184
Specific heat (J/mol. K)	33.8
Thermal expansion ($\times 10^{-6}$/°C)	7.6

1.3 Synthesis method of TMCs and existing problems at present stage

1.3.1 Powder metallurgy (PM)

Powder metallurgy is one of the widely adopted methods for preparing particle reinforced TMCs and is among the earliest applied techniques. This process involves initially uniformly mixing matrix powders with reinforcing particle powders or reactant particles, followed by multiple processes such as compaction, sintering, and hot isostatic pressing to form the material. For instance, Zhang. and Lu. successfully utilized this method to prepare TMCs reinforced with TiC and TiB [13]. However, this method demands high equipment requirements, involves complex procedures, and is particularly challenging to produce large components and mass production.

1.3.2 Self-propagating High-temperature Synthesis (SHS)

Self-propagating high-temperature synthesis (SHS) utilizes the heat released from an exothermic reaction within the system, eliminating the need for an external heat source. While this method offers simplicity and rapid reactions, the process is difficult to control, and the resulting product often exhibits high porosity, necessitating post-processing to eliminate porosity. Researchers like Bazhin P. [14] and Konstantinov A. have successfully employed this method to prepare TMCs reinforced with TiB, showcasing high fracture strength, hardness, and wear resistance.

1.3.3 Reaction hot pressing (RHP)

Reaction hot pressing (RHP) is a processing synthesis method that employs the in-situ formation of reinforcing agents during the hot-pressing process. Researchers such as Geng L. [15] and Ni D. R. have used this method to prepare TiB-reinforced TMCs. Studies by Duygulu O. [16] revealed that RHP produces a three-dimensional mesh structure of reinforcing agents along the matrix grain boundaries, significantly enhancing the strength of the composite material.

1.3.4 Exothermic diffusion method (XDTM)

Exothermic diffusion method (XDTM), originally developed for pre-processing in thermal manufacturing, has been later applied to prepare TMCs. This technique involves mixing reactant powder and matrix alloy powder, forming a uniform mixture, and then heating it to a state of solid-liquid coexistence through an in-situ reaction to create reinforcing agents [17]. Researchers like Zhang Erlin [18] successfully utilized this method to prepare TMCs reinforced with TiC, studying the morphological evolution and distribution of TiC. The results indicated the uniform distribution of TiC particles, consisting mainly of dendritic and equiaxed forms, at both macroscopic and microscopic levels.

1.3.5 Mechanical alloying (MA)

Mechanical alloying is a method where mixed powders undergo solid-state synthesis through impacts and grinding in a ball mill. High-energy ball milling can refine mixed powders to near-nano sizes, activate powder surfaces, enhance mutual diffusion, and induce lattice distortions, resulting in TMCs with exceptional properties [19-20]. Researchers like Miklaszewski A., Jurczyk M. [21] used this method combined with plasma sintering to prepare TiB-reinforced TMCs. They studied the distribution and crystal structure of TiB and its impact on TMCs' performance.

1.3.6 Melting method (MM)

Melting method involves melting the reaction mixture along with titanium alloy matrix raw materials. The heat generated during the melting process facilitates in-situ reactions, forming TMCs. This method allows the preparation of TMCs without changing the conditions of the titanium alloy melting equipment, with in-situ reinforcement generation significantly improving the properties of TMCs [22]. Choi B.J. [23] and Kim I.Y. prepared TiB and TiC enhanced TMC by vacuum induction melting and studied its microstructure and mechanical properties. Choi B.J. 's research shows that the particle size of B4C powder has a significant impact on the properties of composite materials, and the TMC prepared by using finer B4C powder has better properties. They successfully achieved the precision casting of TMC by combining induction melting and precision casting technology, and introduced special powders such as TiO_2, TiAl, Ti_3Al, ZrO_2, Y_2O_3 to prevent the liquid mold reaction of TMC. The wear resistance of TMC prepared by melting method is also analyzed. The results show that the TMC with 20% volume reinforcement rate has the highest volume wear coefficient, and the wear tends to decrease monotonically with the increase of the reinforcement rate [24-25].

1.4 The choice of matrix and reinforcement

1.4.1 The choice of matrix

Based on titanium matrix composites, the content of the matrix far exceeds the content of the reinforcing material. According to the mixing law, the matrix contributes the most to the mechanical properties of the composite, so it is very important to choose the right matrix [26-27]. Titanium alloys are divided into three categories according to their metastable phase structure and the content of β stable elements: α type titanium alloys (pure titanium and near-α high-temperature titanium alloys), β type titanium alloys (near β titanium alloys) and α+β type titanium alloys. After annealing, the microstructure of β-

type titanium alloy is mainly composed of β-phase and has high strength at room temperature. [28-29] However, due to the strict requirements of high temperature properties of materials in the aerospace industry, β-type titanium alloys are almost not selected as the matrix for the preparation of titanium matrix composites. Although β-type titanium alloys can enhance the elastic modulus of composite materials, its application in the aerospace field is limited due to its thermal stability. α+β type titanium alloy combines some advantages of α and β type titanium alloy, with high strength, good toughness and good plasticity, TC4 (Ti6Al4V) is the most widely used titanium alloy [30-31]. However, compared with single-phase α or β titanium alloys, the preparation process of α+β titanium alloys is more complex, requiring more stringent alloy design and heat treatment process. [32] Therefore, the preparation cost of α+β titanium alloys is high, which may limit its application in some fields. α-type titanium alloys, such as TA7, TA11, Ti15, Ti60 and Ti1100, have stable microstructure, good machinability, excellent weldability, good corrosion resistance and high temperature resistance [33]. In this study, α-type titanium alloy was selected as the matrix material, without considering the influence of other metal elements, to study the in-situ reaction mechanism between pure titanium and C-reinforced materials.

1.4.2 The choice of reinforcement

Base alloys are favored for their high modulus, high hardness, high melting point and good high-temperature properties. In order to further enhance its performance, materials in the form of particles or whiskers are usually selected as reinforcement materials. These materials have physical and chemical properties that are compatible with titanium-based alloys and can be added externally or generated by reacting with titanium-based alloys to achieve enhanced effects[34-35].

The criteria for selecting titanium-based alloy reinforcement materials are as follows: (1) Excellent physical properties: the reinforcement material should have good physical properties, such as low density, low melting point and high thermal conductivity, to ensure the lightweight and heat conductivity of the alloy. (2) Good mechanical properties: the reinforcement material should have high modulus and high hardness to improve the strength and wear resistance of the alloy. (3) Good thermal stability: the reinforcement material should have good thermal stability in the titanium matrix and can adapt to the requirements of high temperature treatment, secondary processing, and high temperature use. (4) Thermal expansion coefficient matching: the thermal expansion coefficient of the reinforcement material should be similar to the titanium alloy matrix to avoid stress concentration or thermal stress when the temperature changes. (5) Low solubility: During the processing, the solubility of elements in the reinforcement material should be low to avoid negative effects on the properties of the alloy. (6) Strong binding force: the combination of the reinforcement material and titanium-based alloy should be strong, and the reaction zone between the reinforcement and the matrix alloy should be thin and uniform to ensure the stability and consistency of the enhancement effect [36-38].

Particle reinforcement such as carbide (TiC), borides (such as TiB), nitride (TiN), oxides (such as Al_2O, ZrO) can be used as reinforcement materials, and these particle materials usually have high hardness and high wear resistance. Whisker reinforcement:

such as titanium carbide whisker (TiC whisker), these whisker materials can improve the strength and toughness of titanium matrix composites. Intermetallic compound reinforcement such as Ti_5Si_3, Ti_3Al, TiAl, these intermetallic compounds usually have excellent high temperature strength and corrosion resistance[37, 39]. Table 1.2 shows the physical and mechanical properties of titanium matrix composites that may be used for various ceramic particle reinforcement. [40]

TiC has good thermal compatibility with titanium alloys thermodynamically, can remain stable at high temperatures, and its density is similar to titanium. A change of thermal expansion coefficient of TiC of less than 50% helps to reduce stress concentration due to temperature change. TiC has a Young's modulus of 440 GPa, which is four times that of titanium, while its tensile strength is also much higher than that of pure titanium, helping to improve the strength and rigidity of the alloy[41]. Based on these properties, most old and new research uses TiC as a reinforcement material. Although the density and expansion coefficient of SiC is similar to that of titanium alloy, and its strength is very high, the study found that SiC reinforced titanium-based alloys contain reactants that minimize the interface bonding strength, and the bonding between Al_2O_3 and titanium-based alloys is unstable[42]. TiB has similar thermodynamic properties and similar density to titanium alloys or pure titanium, so it is widely used as a reinforcing material that can be used to strengthen titanium alloys. From the current study, TiC particles and TiB whiskers are suitable for strengthening α titanium alloy or α+β titanium alloy, and TiB_2 is suitable for strengthening TiAl alloy. TiC can also be used to improve the wear resistance of titan-based alloys. The main factor in adding carbon to titanium alloys is the formation of TiC precipitation, which increases the strength of titanium alloys and may be easier to adjust them than through thermal machining. In addition, TiC affects the microstructure and mechanical properties of the alloy[43-45].

Table 1.2 Physical and mechanical properties of reinforcement [40]

Ceramic granules	Density g/cm^3	Melting point ℃	Knoop hardness GPa	Thermal expansion 10^{-6} ℃	Elastic Modulus GPa	Interface bonding and stability
TiC	4.93	3067	28-35	7.74	440	Combined well
TiB	4.57	2200	28	8.6	550	=
TiB_2	4.53	3225	15-45	6.4	529	General Ti Unstable
TiN	5.40	3290	16-20	9.3	250	Combined poor
AlN	3.3	2800	12	564	343	unstable
Al_2O_3	3.97	2054	18-23	8.1	420	unstable
B_4C	2.51	2450	27	4.5	449	unstable
Si**C**	3.21	2697	25	4 63	430	Combined poor

1.5 Advantages and prospects of preparing titanium matrix composites by SPS

SPS (Spark Plasma Sintering) is an advanced powder metallurgy processing technology that sintering metal or ceramic powder particles directly through a pulsed current and effectively apply temporarily generated plasma through a primary axial force to achieve sintering of metal powder at low temperature and within a short period of time [46]. SPS is therefore also referred to as pulsed current sintering (PECS), plasma assisted sintering (PAS) or electric field assisted sintering (EFAS) in some literature [47]. SPS has many advantages over traditional powder metallurgy methods, including high-speed sintering, lower sintering temperature, precise control of sintering energy, and improved density, safety and reliability, especially for the preparation of complex shapes, high-performance metal alloys, ceramic materials and composites. [47] When the spark discharge occurs, the space between the powder particles or the contact surface will melt or evaporate due to local high temperature. This process helps to promote the densification of the composite material, allowing the powder particles to rapidly sintering

and form a dense structure, even at lower temperatures and in a short time [48]. Figure 1.2 shows a schematic of a typical SPS setup. In addition, by using faster heating rates, shorter sintering times and lower sintering temperatures, solidification of metal powders can be achieved without excessive microstructure roughness. In addition, temperature, pressure, and heating rate in SPS technology are the main parameters controlling microstructure characteristics such as grain size, grain boundary mismatch distribution, and lattice position. This shows that the SPS technology is able to precisely adjust the microstructure of the material by controlling these parameters, thus achieving fine adjustment of the properties of the final product [49]. There are three main mechanisms for enhancing SPS technology [50-51]: (i) Applying pressure: The pressure applied during the SPS process helps to promote the bonding between powder particles, thereby enhancing densification and formation during sintering. (ii) Heat generation through the Joule effect: in the SPS process, through the conduction of electric current in the conductive powder particles, the resulting resistance leads to the Joule effect, which generates heat and promotes the heat treatment and sintering of the particles. (iii) Generation of plasma in the interstitial and surface of conductive powder particles: The high pulse current density generates plasma in the interstitial and surface of the powder particles, which helps to remove contaminants and oxide layers on the surface of the particles, and enhances the mass transfer between the particles, thus further facilitating the sintering process. In general, as a new sintering technology, SPS has a wide range of application prospects in the field of material processing, especially for the preparation of complex shapes, high-performance metal alloys, ceramic materials and composite materials. [52]

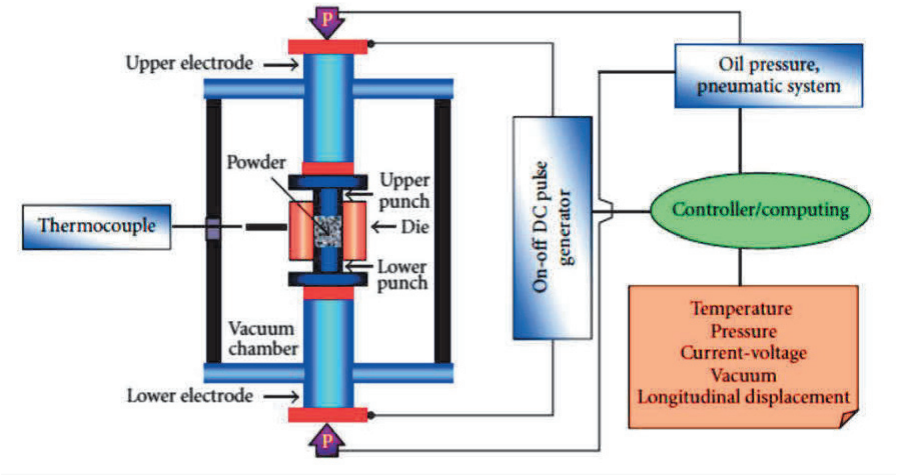

Fig. 1.2 Schematic view of SPS.

1.6 Problem of previous studies and objectives of this study

In summary, TMCs have gained significant attention due to their outstanding properties, including high-temperature resistance, high modulus, high strength-to-weight ratio, and customizable performance, especially in high-tech fields such as aerospace. These characteristics make titanium matrix composites widely applicable in the aerospace industry. With the advancement of technology and in-depth research, higher demands have been placed on the performance and manufacturing cost of structural titanium materials. Traditional titanium alloys have reached their limits in certain aspects of performance and improving the mechanical properties solely through changes in alloy elements, content, or heat treatment processes has become challenging, restricting further applications of titanium materials. Non-continuous reinforced titanium matrix composites, with advantages such as isotropy, significant economic benefits, and broad market prospects, have become a hot research topic in the field of titanium. Although the addition of reinforcement improves strength, it results in a significant reduction in room temperature ductility. Good ductility allows materials to undergo prolonged deformation before fracture, avoiding significant losses due to sudden failure, ensuring the safety of service, and facilitating subsequent processing. Therefore, the development of high ductility titanium matrix composites is urgently needed.

For titanium matrix composites, the rational selection of preparation methods is crucial to obtaining high-performance materials. In recent years, the preparation methods for TMCs have mainly included mechanical alloying (MA), powder metallurgy (PM), and ingot metallurgy (IM) techniques. However, these methods have their own advantages and disadvantages, such as uneven distribution of TiC particles, extremely high sintering temperatures, and complex heat treatment processes. Additionally, most studies have focused too much on performance improvement, neglecting the importance of preparation cost. For instance, using expensive spherical titanium powder as the matrix material to

reduce powder oxygen content, employing inefficient and hazardous high-energy ball milling for refining, and solving the insufficient driving force for coarse powder sintering through costly discharge plasma sintering with short mold lifespans and difficulties in mass-producing large-sized components. Despite the potential benefits of high-temperature plasma sintering, many preparation processes remain at the laboratory stage, posing significant challenges to the further development of titanium matrix composites.

Therefore, our research aims to adopt a low-cost and industrially feasible preparation route, achieving a technological breakthrough in the in-situ preparation of titanium matrix composites. This approach aims to overcome issues such as uneven distribution of the reinforcement phase in the matrix, poor interface performance, and low ductility. Our study, combining in-situ synthesis technology and hot-pressing, produced TiC-reinforced titanium matrix composites using layered graphite paper as a carbon source, clarifying the presence forms and reinforcement mechanisms of carbon atoms in the matrix. The research results validate the feasibility of layered stacking to prepare high-performance, high-ductility titanium matrices. We systematically studied the influence of different reinforcement phase amounts on product distribution, microstructural evolution, and mechanical properties, exploring the mechanism of reinforcement phase generation. Additionally, an analysis of the microstructural evolution and reinforcement mechanism of samples was conducted to obtain high-ductility titanium matrix composites.

1.7 Outline of this study

Chapter 1 introduces the structure of TiC and the classification and preparation methods of TMCs and provides a review of the development of advanced TMCs. The requirements properties of TMCs and the problems of the existed TMCs were also discussed.

Chapter 2 the microstructure evolution during the fabrication of in situ TiC reinforced TMCs has been investigated. By observing the structure of the produced composite material, the state of dispersion of the base metal structure and reinforcing material have been investigated in this chapter.

Chapter 3 ultra-thin graphite powder sheets made of graphite powder and PVA were used as a carbon source for the laminated sintering. In addition, the microstructural evolution during the fabrication of in-situ TiC-reinforced TMCs was investigated with a particular focus on the formation mechanism of rod-like TiC particles. Tensile tests were carried out as an assessment of the mechanical properties.

In Chapter 4, our primary objective is to ensure a comprehensive in-situ reaction and uniform distribution of reinforcement within Ti/C composites containing varying carbon contents. We achieve this by employing ultra-thin graphite powder sheets as the carbon source and 0.05 mm thick titanium foil as the titanium matrix through a layer-stacked sintering method. Additionally, the effects of carbon content on the morphology of the reinforcement, the evolution of the microstructure of the matrix and the mechanical properties of the composites were systematically investigated through composition design and process optimization.

As last, the results from the above-mentioned studies are summarized in Chapter 5.

References

[1] Saito, T.: Advanced Performance Materials, **2** (1995) 121-144.

[2] Liu Y., Chen L. F., Tang H. P.: Materials Science and Engineering: A, **418** (2006) 25-35.

[3] R. Ye, H. Huang: 2021 IEEE International Conference on Electronic Technology, Communication and Information (ICETCI), (2021) 284-289.

[4] Tjong S C, Mai Y W.: Composites science and technology, **68** (2008) 583-601..

[5] Kan Y. Y., Su F. Z., Xu. X.R.: Shanghai Chemical Industry, **48** (2023) 58-61.

[6] Sun J., Qi Y. J., Liu H.: Journal of Materials Protection, **53** (2020) 151-156.

[7] Liu R. Z., Luo G.Z., Lai X. J.: World Nonferrous Metal, (2000) 42-45.

[8] Hang Y., Lee Y. J., Chang S.: International Journal of Machine Tools and Manufacture, **174** (2022) 103851.

[9] Sun P., Fang Z. Z., Zhang Y.: Jom, **69** (2017) 1853-1860.

[10] Lye R. G., Logothetis E. M.: Physical Review, **147** (1966) 622.

[11] Miracle D. B., LIPSITT H. A.: Journal of the American Ceramic Society, **66** (1983) 592-597.

[12] Mhadhbi M., Driss M.: J. Brill. Eng, **2** (2021)1-11.

[13] Zhang X., Lü W., Zhang D.: Scripta materialia, **41** (1999) 39-46.

[14] Bazhin P., Konstantinov A., Chizhikov A.: Materials Today Communications, **25** (2020) 101484.

[15] Geng L., Ni D. R., Zhang J.: Journal of Alloys and Compounds, **463** (2008) 488-492.

[16] Duygulu O.: Met. Mater, **56** (2018) 265-275.

[17] Mitra R., Chiou W. A., Weertman J. R.: MRS Online Proceedings Library (OPL), **238** (1991) 871.

[18] Zhang E., Songyan Z., Zhu Z.: Journal of materials science, **35** (2000) 5989-5994.

[19] Feng H. B., Jia D. C., Zhou Y.: Materials science and technology, **20** (2004) 1205-1210.

[20] W. X. Chu, P. H. Tseng, C. C. Wang: Appl. Therm. Eng. **163** (2019) 114438.

[21] Miklaszewski A., Jurczyk M.: Materials, **12** (2019) 653.

[22] Feng H. B., Jia D. C., Zhou Y.: Materials science and technology, **20** (2004) 1205-1210.

[23] Lian G., Zhang H., Zhang Y.: Materials, **12** (2019) 793.

[24] Choi B. J., Kim Y. J.: Metals and Materials International, **19** (2013) 1301-1307..

[25] Choi B. J., Kim Y. J.:Materials Transactions, **52** (2011) 1926-1930.

[26] Ammisetti D.K., Kruthiventi S. S. H.: Materials Today: Proceedings, **46** (2021) 9730-9735.

[27] Ward-Close C. M., Minor R., Doorbar P. J.: Intermetallics, **4** (1996) 217-229.

[28] Ezugwu E. O., Wang Z. M.: Journal of materials processing technology, **68** (1997) 262-274.

[29] Kolli R. P., Devaraj A.: Metals, **8** (2018) 506.

[30] Froes F. H., Bomberger H. B.: Jom, **37** (1985) 28-37.

[31] Disegi J. A., Roach M. D., McMillan R. D.:Journal of Biomedical Materials Research Part B: Applied Biomaterials, **105** (2017) 2010-2018..

[32] Xu J., Zeng W., Zhang X.: Journal of Alloys and Compounds, **788** (2019) 110-117.

[33] Semiatin S. L., Seetharaman V., Weiss I.: Jom, **49** (1997) 33-39.

[34] Zhang X., Song F., Wei Z.: Materials Science and Engineering: A, **705** (2017) 153-159.

[35] Zhang C. J., Kong F. T., Xiao S. L.: Materials Science and Engineering: A, **548** (2012) 152-160.

[36] Moongkhamklang P., Elzey D. M., Wadley H. N. G.: Composites Part A: applied science and manufacturing, **39** (2008) 176-187.

[37] Yang H., Chen X., Huang G.: Journal of Magnesium and Alloys, **10** (2022) 2311-2333.

[38] Li G., Munir K., Wen C.: Journal of Manufacturing Processes, **56** (2020) 131-146.

[39] Shetty R., Hegde A., Shetty SV. U. K.: Journal of Composites Science, **6** (2022) 88.

[40] Gofrey T. M. T., Goodwin P. S., Ward‐Close C. M.: Advanced Engineering Materials, **2** (2000) 85-91.

[41] Das K., Bandyopadhyay T. K., Das S.: Journal of materials science, **37** (2002) 3881-3892.

[42] Wang Y., Zhang G., Zhang X,.: Acta Metall Sin, **5** (2016) 1153-1170.

[43] Delbari S. A., Namini A. S., Asl M. S.: Materials Today Communications, **20** (2019) 100576.

[44] Ma F., Wang C., Liu P.: Journal of Alloys and Compounds, **758** (2018) 78-84.

[45] Lee W. H., Seong J. G., Yoon Y. H.: Ceramics International, **45** (2019) 8108-8114.

[46] Xiong Y., Du M., Zhang F.: Journal of Alloys and Compounds, **886** (2021) 161216.

[47] Jeje S. O., Shongwe M. B., Rominiyi A. L.: The International Journal of Advanced Manufacturing Technology, **117** (2021) 2529-2544.

[48] Poletaev G. M., Sitnikov A .A., Yakovlev V. I.: Journal of Experimental and Theoretical Physics, **134** (2022) 183-187.

[49] Feng H., Jia D., Zhou Y.: Composites Part A: Applied Science and Manufacturing, **36** (2005) 558-563.

[50] Meir S., Kalabukhov S., Frage N.: Ceramics International, **41** (2015) 4637-4643.

[51] Mohammadzadeh A., Namini A. S., Azadbeh M.: Materials Research Express, **5** (2018) 126512.

[52] Singh N., Ummethala R., Karamched P. S.: Journal of Alloys and Compounds, **865** (2021) 158875.

Chapter 2

Fabrication of In-Situ TiC Particles reinforced Ti Matrix Composites with graphite powder sheets

2.1 Introduction *23*

2.2 Experimental procedure *25*

2.2.1 Raw materials *25*

2.2.2 Fabrication of graphite powder sheet *25*

2.2.3 Reaction of single layer of graphite powder sheet and Ti plates *26*

2.3 Results and discussion *27*

2.3.1 Microstructures *27*

2.3.2 TiC reaction rate and mechanism *30*

2.3.3 Diffusion mechanism of titanium carbide *33*

Summary *34*

References *35*

2.1 Introduction

As a structural material, titanium alloy has the ideal characteristics of light weight, high strength and corrosion resistance [1-3]. Due to these unique properties, it has gradually established market demand in the aviation sector and is widely used in the manufacture of aircraft engines and structural components [4]. Figure 2.1 vividly shows the evolution of the weight ratio in the aircraft structure. As can be seen from the description in Figure 2.1, the demand for titanium in the aviation sector is expanding year by year. At present, the aviation industry's focus on resources, environment and energy is inevitable. As the number of aircraft increases, improving fuel efficiency becomes particularly important [5-7]. Achieving lightweight and improving engine efficiency are effective ways to promote aircraft fuel efficiency, which in turn drives the expected growth in demand for titanium. In addition, titanium with its excellent mechanical properties, corrosion resistance and biological adaptability, not only has a wide range of applications in the field of aviation, but also covers the Marine, medical, sports equipment and fashion and other fields. The demand for titanium in these different areas is gradually increasing every year [8-10].

However, titanium also faces some challenges, such as low wear resistance. Because of its excellent mechanical properties and active metal properties, the manufacture of titanium alloys has become very complicated [11]. Its alloy manufacturing requires high energy consumption and precision manufacturing processes, so how to reduce costs and improve production efficiency is still a key issue. In addition, titanium alloys also have some problems with wear resistance and specific rigidity, and as the need for reliability increases, improving these properties becomes even more critical [12-13].

Traditionally, the improvement of metal material properties is mainly achieved through alloying. In recent years, however, there has been a growing interest in composite materials that combine metals as substrates with ceramics as strengthening materials [14]. The preparation process of the composite material is shown in the figure, as if the two

were mixed into one in the expectation of a superimposed effect on its properties. This class of new materials prepared from composite materials is defined as composite materials with superior properties, by artificially combining two or more different materials, to achieve properties that cannot be achieved by a single material, and to meet specific needs [15]. Titanium matrix composites are expected to be an alternative to titanium alloys by improving wear resistance and specific rigidity while retaining the light, strong and corrosion resistant properties of titanium. With the development of low-cost manufacturing processes for titanium matrix composites, we expect to be able to further promote their widespread alternative applications in fields such as aviation [16]. In this study, we investigated the microstructure evolution during the preparation of in situ TiC strengthened TMC. By observing the structure of the composites produced, the dispersion state of the base metal structure and the reinforcing material was investigated.

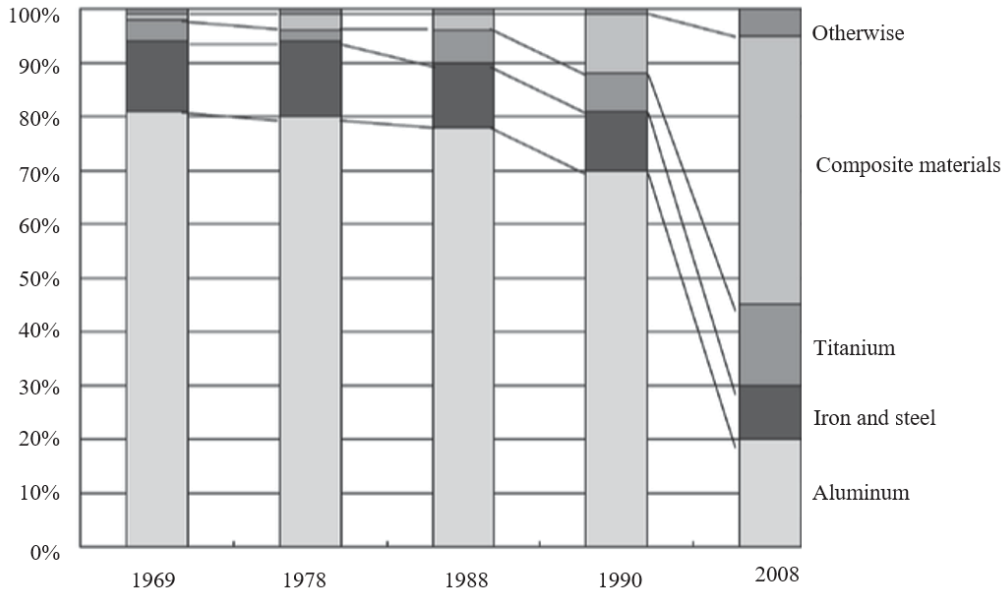

Fig. 2.1 Composition weight ratio of the civil aviation aircraft

2.2 Experimental procedure

2.2.1 Raw materials

In this study, pure Ti plates (>99.49%, 1mm thick), graphite powder (>90%, 5μm), and PVA solution (polyvinyl alcohol, 13 wt%) were used as starting materials. The detailed properties of pure titanium are listed in Table 2.1.

Table 2.1. Properties of pure titanium.

Thickness t (mm)	Purity (%)	Tensile strength σ_{TS}/ (MPa)	Yield strength σ_{YS}/ (MPa)	Elongation δ (%)
1	>99.49	320	165	27

2.2.2 Fabrication of graphite powder sheet

The graphite powder sheet as the carbon source was prepared as follows (shown in Figure 2.2): 0.3125g graphite powders were mixed in 12.5g PVA solution (13 wt %) in a beaker and continuous stir at 323K for 1h to form a homogeneous solution. The resultant solution was rolled evenly on a transparency film and then put in a drying oven to evaporate the solvent at 343K for 24h. The thickness of the resultant graphite powder sheet is about 20μm.

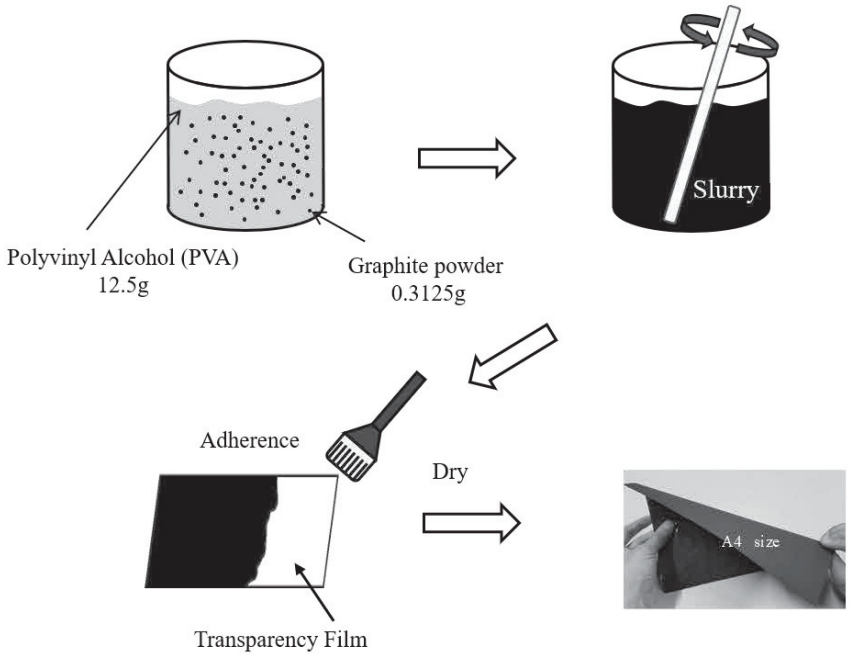

Figure 2.2. Schematic illustration of fabricating processes of Graphite powder sheet.

2.2.3 Reaction of single layer of graphite powder sheet and Ti plates

Two Ti plates and one graphite powder sheet were cut into ϕ10 mm disks and then use fine quartz sandpaper to remove the oxide film on the surface of Ti plates. One piece of graphite powder sheet was sandwiched by two pieces of Ti plates and then sintered in a spark plasma sintering (SPS) furnace at 873K, 973K, 1073K, 1173K, and 1273K, respectively, under 50MPa for 0.6k s to investigate the amount of reaction production (TiC) between graphite powder sheets and Ti plates with different sintering temperature.

Microstructures of composites are revealed by Scanning Electron Microscope (SEM, TOPCON SM-520, Japan). The powder morphology and sintered microstructure were observed by Electron Probe Micro-Analyzer (EPMA, JXA-8900, Japan). X-ray diffraction (XRD; D/max-2500/PC, Japan) analysis was carried out using Cu Kα radiation (λ = 1.54056 Å) at a scanning speed of 1° /min over the 2θ range of 30°-75°.

2.3 Results and discussion

2.3.1 Microstructures

To observe the process of titanium-carbon diffusion reaction, a set of samples with different sintering temperatures was prepared. Figure 2.3(a)-(e) shows the vertical section of single-layer Ti matrix composite. Figure 2.3(a')-(e') are replication views of the residual graphite sheet after sintering. At the sintering temperature of 873K, almost no reaction was observed at the bonding area between the two titanium plates and the graphite powder sheet. At the sintering temperature of 973 K and above, it can be observed macroscopically that the titanium plates bonded together, and the bonding area increased as the sintering temperature increased. When the sintering temperature was increased to 1273K, about 95% of the graphite sheet reacted with titanium plates.

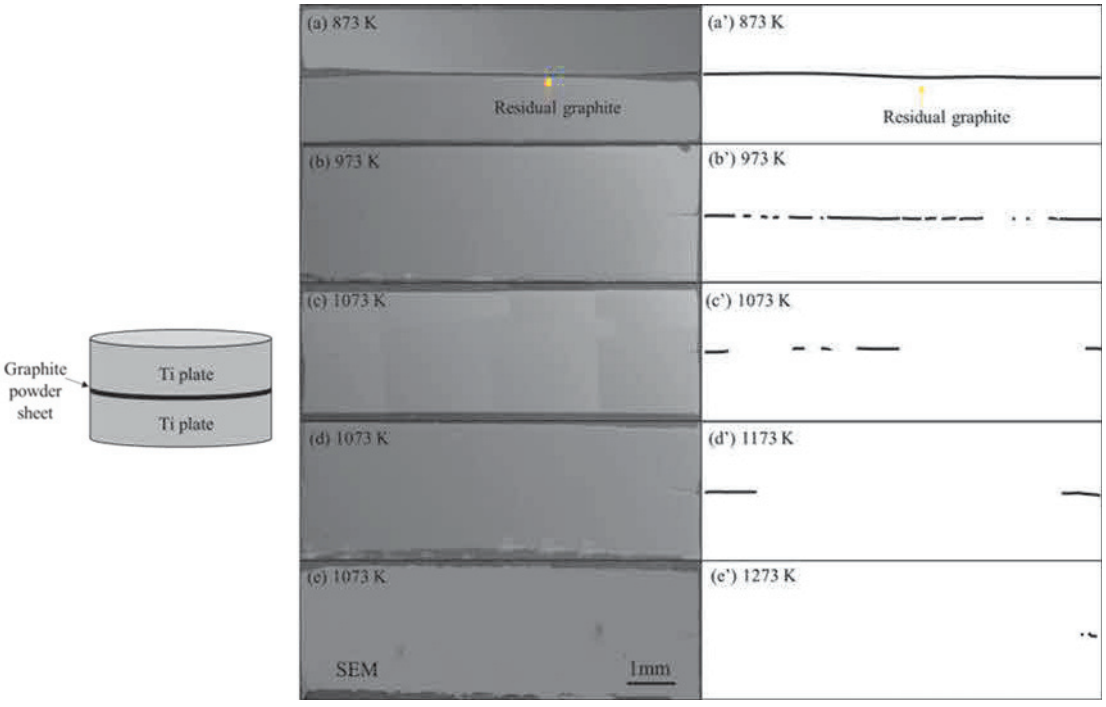

Figure 2.3. SEM images of Ti matrix composite by different of sintering temperature: 873K(a), 973K(b), 1073K(c), 1173K(d) and 1273K (e); (a')-(e'): Corresponding replication view of the residual graphite.

At microscopic view, the reaction process is shown in Figure 2.4. BSE image and area mapping of the sample with sintering temperature of 1073K is shown in Figure 2.4(a). A dark gray interlayer can be seen at the interface of remained graphite and titanium plates, which is considered to be TiC. In some places, two titanium plates bond together, which is probably caused by the uneven thickness of graphite powder sheet. When the sintering temperature was increased to 1273K, as shown in Figure 2.4(b), most of the graphite layer disappeared, but some short gray lines were observed at the original graphite powder sheet positions. In addition, many gray particles interspersed around the original graphite powder sheet position, but there are few particles presenting away from the center.

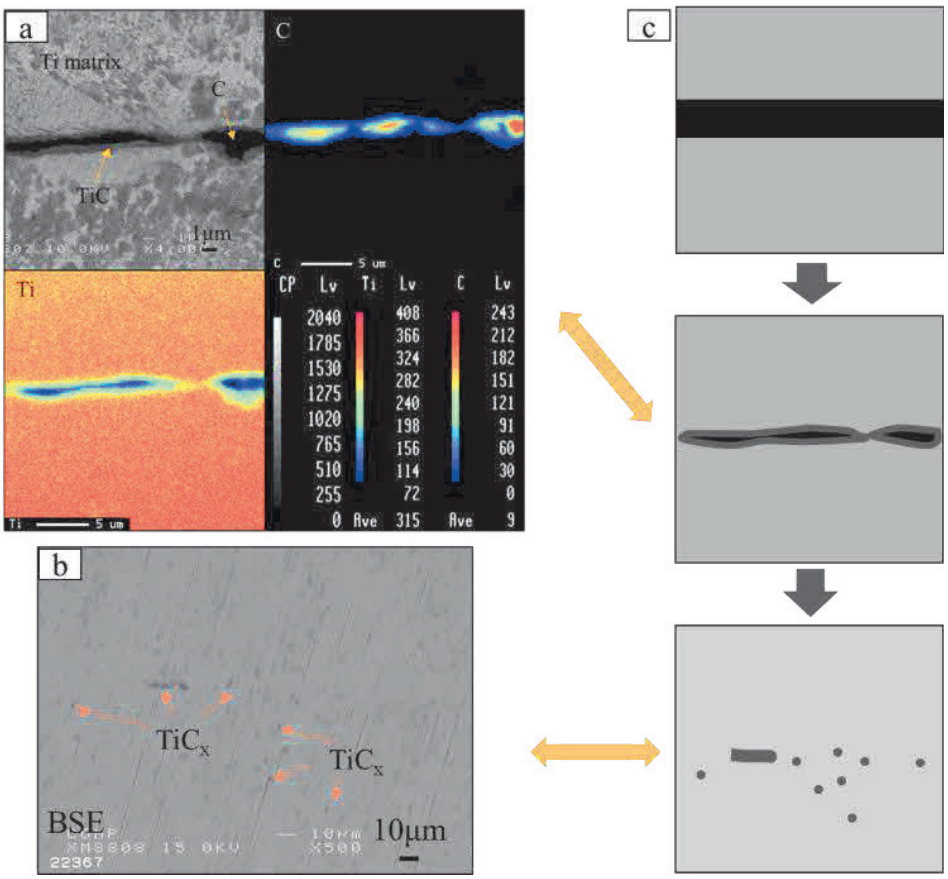

Figure 2.4. (a) BSE image and area mapping by EPMA of bonding area of TMC of 1073 K; (b) BSE image of TMC of 1273 K; (c) Schematic illustration of synthetic process of in-situ TiC particles dispersed TMC.

To analyze the gray particles formed in the matrix, an FE-SEM image and EDS point analysis on these gray particles are shown in Figure 2.5. As the results of point analysis, the dark gray particles are determined to be TiCx particles. These TiC particles have an average particle size of 1 μm. Besides, the standard free energy ΔG of TiC formation was calculated by following equation when the sintering temperature is lower than 1973K [12]:

$$\Delta G = -184571.8 + 41.382T - 5.042T\,lnT + 2.425 \times 10^3\,T^2 - 9.79 \times 10^5/T \quad (T < 1939K) \quad (2.1)$$

The Gibbs free energy ΔG for the reaction of titanium and graphite at 1073K and 1273 K can be calculated as -172 kJ/mol and -174 kJ/mol, respectively. This result indicated the formation of TiCx at 1073K and 1273K is spontaneous generation. Figure 4(c) is a schematic diagram of the diffusion-reaction between graphite and titanium matrix with increasing temperature.

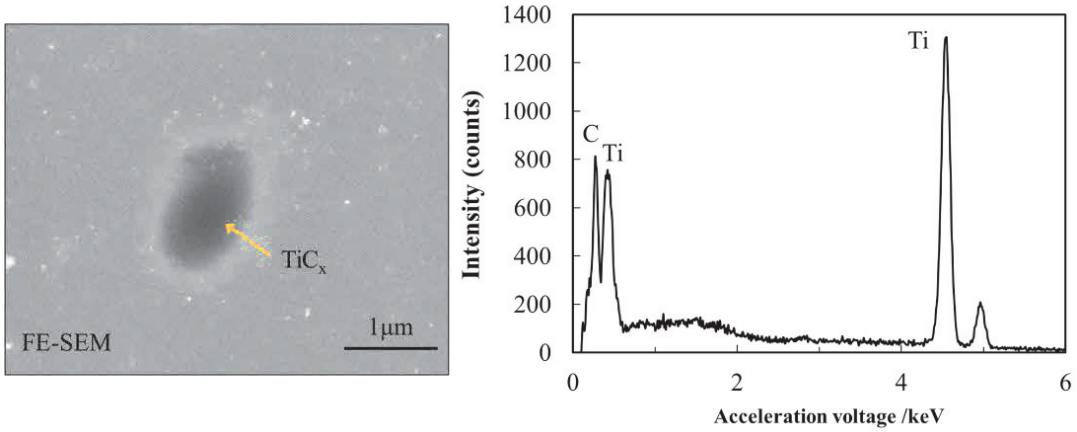

Figure 2.5. FE-SEM image and point analysis by EDS of TiC reinforced TMC sintered at 1273 K.

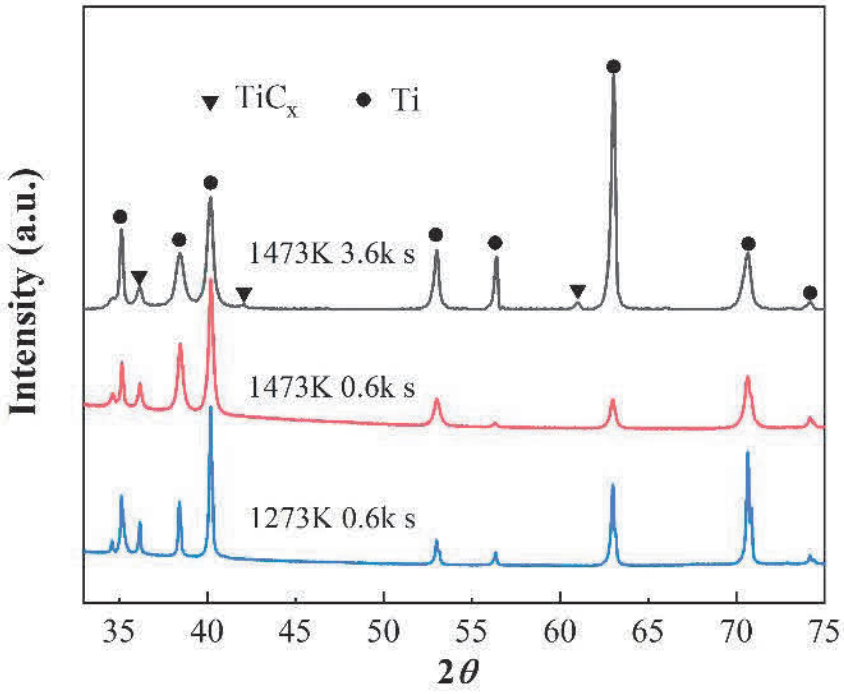

Figure 2.6. XRD pattern of TiC reinforced TMC sintered with different sintering temperature.

Figure 2.6 shows XRD patterns. It is evident from the Figure that each composite consists of TiC and hexagonal close-packed (HCP) α-Ti.

2.3.2 TiC reaction rate and mechanism

Chemical reaction refers to the process of breaking the bond of reactants, forming a new bond, and thus producing a product [16]. To initiate a chemical reaction, enough energy must be provided to the reactants in order to break or form a bond, so a certain amount of time is required. In order to trigger this reaction, it is necessary to apply conditions exceeding a certain energy, so that the chemical bond is easily broken into an active state, and this minimum energy required is called the activation energy. In order to reduce the activation energy, that is, to increase the reaction speed, some methods can be taken, such as increasing the concentration of reactants, increasing the temperature, adding catalysts, etc. In this study, we confirm that as the sintering temperature increases, titanium and carbon react and the amount of unreacted carbon decreases.

$$k = Aexp\left(\frac{-E_a}{RT}\right) \quad (2.2)$$

The reaction rate constant is a value that expresses the rate of increase or decrease of the reactants in a chemical reaction. The rate constant k can be obtained by Arrhenius equation [17]. Taking the natural logarithm of both sides of Arrhenius's equation, it can be expressed as a first order equation. Then, plot the graph with ln(k) as the vertical axis and 1/T as the horizontal axis to obtain the "Arrhenius diagram" shown in Figure 2.7. The reaction rate constant k and temperature T are values that can be measured experimentally, and the activation energy *E*a can be experimentally obtained from the slope of the diagram.

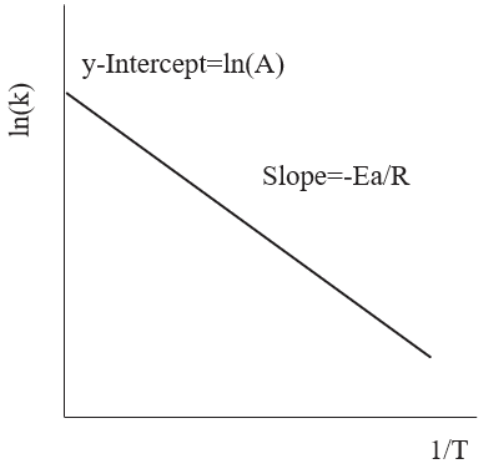

Fig. 2.7 Image of Arrhenius plot.

The following is a summary of the results of experiments conducted by Lee J. H. and Thadhani N. N, studying the reaction rates of titanium and carbon [17-18]. The activation energy of titanium and carbon forming TiC is 29~47 kcal/mol, and the activation energy of carbon diffusing into titanium through the TiC interface is about 100 kcal/mol, which is 2~3 times lower than the reaction rate of TiC. In addition, the activation energy of titanium mediated into carbon through the TiC interface is 176 kcal/mol, which is 4 to 6 times lower than the reaction rate of TiC. These results are graphically presented in Figure 2.8. In general, when titanium and carbon begin to react, the first carbon will diffuse to

the titanium side, forming a TiC. The carbon then diffuses as carbon through the carbide TiC interface.

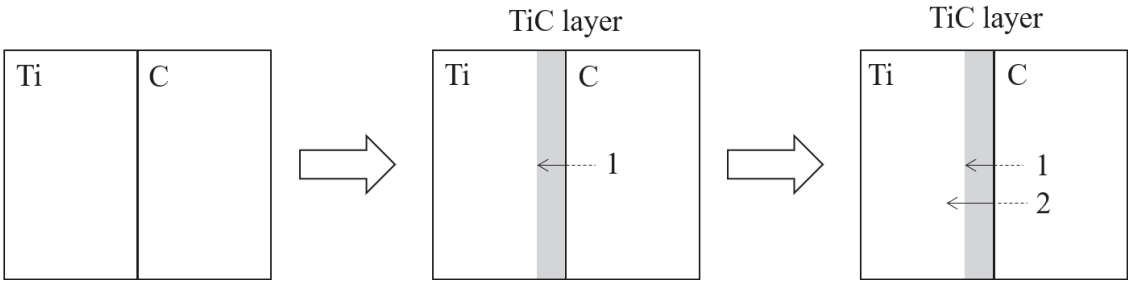

Fig. 2.8 Schematic illustration of solid-state reaction mechanisms in Ti and C diffusion-couple.

2.3.3 Diffusion mechanism of titanium carbide

The C and Ti atoms diffuse to the bonding surface of the titanium layer and the graphite paper, and the TiC compound is formed by in-situ reaction. The reaction layer forms TiC atoms by diffusion. After the chemical reaction takes place, the TiC atoms formed further form TiC particles through diffusion. The nucleation of TiC compounds begins when the nucleation capacity of TiC compounds is greater than the critical power required for nucleation. When the nucleation capacity of TiC particles reaches a certain level, they begin to form under the right conditions and begin to grow. From the crystal structure of TiC, the placeholders of Ti and C atoms show a completely centrosymmetric structure, which indicates that TiC particles have a certain symmetry. Because of this symmetry, TiC particles are likely to form equiaxial spherical particles. The liquid-solid interface is easy to achieve tissue supercooling during the solidification process, and TiC particles will grow dendritic shape due to the existence of supercooling. Dendritic, as a primary TiC, is easy to grow into strips or rods in the supercooled melt. The nucleation rate of TiC particles is greater than the growth rate due to the large degree of supercooling at the liquid-solid interface. TiC particles often show uniform and fine characteristics when formed in liquid titania-based alloys. [12, 19].

Summary

(1) A manufacturing process was developed for producing particle-reinforced titanium-based composite materials using titanium plates and graphite powder sheets.

(2) Graphite powder sheet and titanium plates were bonded together due to the solid phase reaction over 973K. The bonding area increased as the temperature increased. The bonding rate was up to 95% at sintering temperature of 1273 K.

(3) By using EPMA surface analysis FE-SEM point analysis, TiC particles with an average diameter of 1μm were observed in the Ti matrix nearby the original position of graphite powder sheet and it can be determined that the gray line appeared in the junction of GPs and titanium matrix is TiC and residual graphite.

References

[1] Pandey U., Purohit R., Agarwal P.: Materials Today: Proceedings, **4** (2017) 5452-5460.

[2] Li S., Sun B., Imai H.: Carbon, **61** (2013) 216-228.

[3] Zhang Y., Sun J., Vilar R.: Journal of Materials Processing Technology, **211** (2011) 597-601.

[4] Hayat M. D., Singh H., He Z.:Composites Part A: Applied Science and Manufacturing, **121** (2019) 418-438.

[5] Leyens C., Hausmann J., Kumpfert J.: Advanced Engineering Materials, **5** (2003) 399-410.

[6] Singerman S. A., Jackson J. J., Lynn M.: Sup eralloys, **3** (1996) 579-586.

[7] Attar H., Ehtemam-Haghighi S., Kent D.: International Journal of Machine Tools and Manufacture, **133** (2018) 85-102.

[8] Abkowitz S., Abkowitz S. M., Fisher H.: Jom, **56** (2004) 37-41.

[9] Ward-Close C. M., Winstone M. R., Partridge P. G.: Materials & Design, **15** (1994) 67-77.

[10] Huang L., An Q., Geng L.: Advanced Materials, **33** (2021) 2000688.

[11] Zhang X., Yu W., Wang J: Vacuum, **207** (2023) 111635.

[12] Wei W. H., Shao Z. N., Shen J.: Materials Science and Technology, **34** (2018) 191-198.

[13] C. P. Feng: Compos. Commun. **22** (2020) 100528.

[14] Lee W. H., Seong J. G., Yoon Y. H.: Ceramics International, **45** (2019) 8108-8114.

[15] Huang L. J., Geng L., Xu H. Y.: Materials Science and Engineering: A, **528** (2011) 2859-2862.

[16] Attar H., Ehtemam-Haghighi S., Kent D.: International Journal of Machine Tools and Manufacture, **133** (2018) 85-102.

[17] J. K. Ma: Chem. Eng. J. **380** (2020) 122550.

[18] A. Marconnet, N. Yamamoto, M. A. Panzer, B. L. Wardle: ACS Nano, **5** (2011) 4818-4825.

[19] Fan S., Zhong L., Xu Y.: Advanced Engineering Materials, **17** (2015) 1562-1567.

Chapter 3

Fabrication of In-Situ Rod-like TiC Particles Dispersed Ti Matrix Composite

3.1 Introduction *38*

3.2 Experimental procedure *40*

3.2.1 Raw materials *40*

3.2.2 Fabrication of graphite powder sheet *40*

3.2.3 Fabrication of TMCs with multi-layer graphite powder sheets *41*

3.2.4 Hot forging of composite materials *43*

3.3 Results and discussion *44*

3.3.1 XRD *44*

3.3.2 Microstructure *45*

3.3.3 Tensile testing and strengthening mechanism analysis *49*

Summary *53*

References *54*

3.1 Introduction

Titanium and its alloys have excellent mechanical properties, corrosion resistance and relatively low density, and are therefore widely used in structural applications in aerospace, defense, automotive and other industries. However, there are deficiencies in the elastic modulus, hardness and wear resistance of titanium alloys, which limit their wider application [1-6]. In order to overcome these shortcomings, the introduction of strong ceramic phase to manufacture TMC is an effective strategy. TMC has received much attention because of its excellent properties, including high elastic modulus, high strength, good creep and fatigue resistance at high temperatures. This makes TMC have broad application prospects in aerospace industry, biomedical care industry, energy power generation industry, petrochemical industry and other fields [1-4]. Researchers are committed to exploring titanium-based composites to provide superior properties and performance. As one of the best reinforcement materials, TiC has wear and corrosion resistance and is often used to strengthen TMC. TiC enhanced TMCS typically have excellent wear resistance, tensile strength and corrosion resistance [2-4].

As well known, it has been found that the mechanical properties of TMCs mainly depend on the composition and microstructure of the matrix and reinforced particles [7]. The in-situ synthesis method refers to the synthesis of reinforcing materials in the matrix by utilizing the reaction between the reactants and the alloy matrix. The in-situ fabrication technique is considered to be one of the most promising methods for preparing titanium matrix composites in the matrix due to the fine size and the strong interfacial bonding between the matrix and the reinforcement phase [3]. In situ synthesis method refers to the method of synthesizing reinforcement materials in the matrix by the reaction between the reactants and the alloy matrix. In situ preparation technology is considered as one of the

most promising methods for preparing titanium matrix composites in matrix because of its good size and interface bonding ability between reinforced phases. In-situ technology is easy to manufacture and low cost, so it is receiving more and more attention [8]. The selection of compatible reinforcement materials is important for the development of particle reinforced TMC. TMC uses a variety of high-modulus ceramic reinforcement materials, such as SiC, TiB, Al_2O_3 and TiC. Among these reinforcement materials, TiC is considered to be one of the best reinforcement materials for TMC due to its excellent properties. TiC has the characteristics of high hardness, high modulus and high bending strength, and is a suitable candidate for use as a wear-resistant TMC reinforcement phase. [5, 9]. TiC has a face-centered cubic (FCC) nacl-type structure, and its composition is generally non-stoichiometric, expressed as TiCx, where x is the ratio of C to Ti, ranging from 0.46 to 0.98. Traditional TMC preparation methods include powder metallurgy (PM), melting (MM) and mechanical alloying (MA) [11-12]. Powder metallurgy by mixing titanium powder and reinforced phase, through pressing molding, sintering and other processes to cure into composite materials. The melting method is to heat titanium and the reinforced phase to their melting point at ultra-high temperatures, and then rapidly cool to form a composite material. Mechanical alloying is to mix the titanium powder and the reinforced phase by ball milling in a high-energy ball mill, so that it is evenly mixed at the microscopic level, and then the powder is cured by hot pressing or hot isostatic pressing. These traditional methods have advantages and disadvantages, among which the uneven distribution of TiC particles, high sintering temperature and complex heat treatment process are the main disadvantages. In order to overcome these problems, the lamination sintering technology was used to prepare the composite with microlayered structure, which has the advantages of uniform distribution, simple preparation process and strong interface bonding force[11-13]. In this study, titanium matrix composites (TMC) were prepared on the alternating stack of titanium foil and graphite powder by hot pressing sintering method. In order to ensure that the graphite layer can be fully diffused

into the titanium matrix, an ultra-thin graphite powder sheet made of graphite powder and PVA is used as a carbon source for lamination sintering. In this study, we focuse on the microstructure evolution of in-situ TiC enhanced TMC preparation, with special attention to the formation mechanism of rod-like TiC particles. This is to gain a deeper understanding of the generation process and structural characteristics of TiC in TMC. Tensile tests are used to evaluate the mechanical properties of TMC to understand important properties such as strength and toughness of the material.

3.2 Experimental procedure

3.2.1 Raw materials

In this study, pure Ti foils (>99.49%, 0.1mm thick), graphite powder (>90%, 5μm), and PVA solution (polyvinyl alcohol, 13 wt%) were used as starting materials. The detailed properties of pure titanium are listed in Table 1.

3.2.2 Fabrication of graphite powder sheet

The graphite powder sheet as the carbon source was prepared as follows (shown in Figure 3.1): 0.3125g graphite powders were mixed in 12.5g PVA solution (13 wt %) in a beaker and continuous stir at 323K for 1h to form a homogeneous solution. The resultant solution was rolled evenly on a transparency film and then put in a drying oven to evaporate the solvent at 343K for 24h. The thickness of the resultant graphite powder sheet is about 20μm. As shown in Figure 3.1(a), the graphite powder sheet shows smooth and uniform in texture.

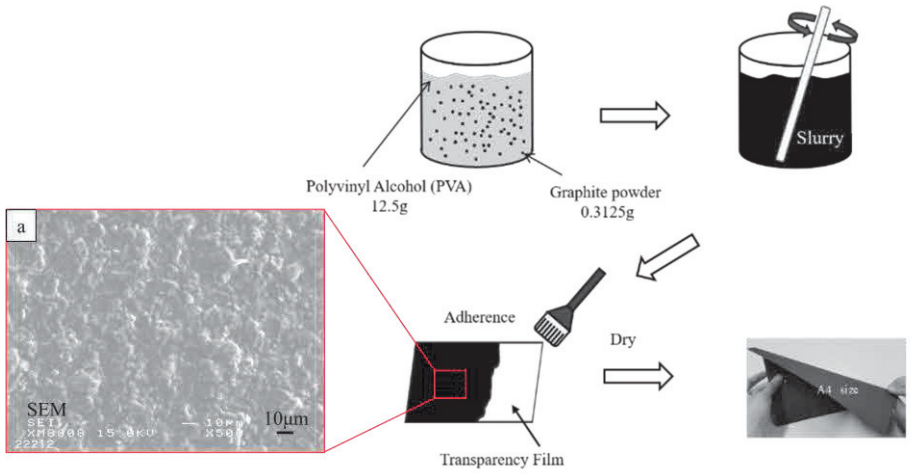

Figure 3.1. Schematic illustration of fabricating processes of Graphite powder sheet: (a) the SEM image of graphite powder sheet.

3.2.3 Fabrication of TMCs with multi-layer graphite powder sheets

Ti plate, Ti foils, and graphite powder sheets were cut into ϕ10 mm disks and then the Ti plates and foils were cleaned in the ultrasonic bath of acetone for the 1.2k s. Then, two thick Ti plates are placed on the top and bottom ends, alternating between one piece of graphite powder sheet and one pieces of titanium foil in the middle as shown in Figure 3.2(a). A total of 10 pieces of graphite powder sheet and 9 pieces of titanium foil were used. The mass fraction of graphite is 0.82 wt %. LBN spray (ingredients: methyl ethyl ketone, dimethyl ether, isopropyl alcohol, nitrocellulose, manufactured by Showa Denko) was used as release agent. And then the samples were sintered in a spark plasma sintering (SPS) at 1273K under 50MPa for 0.6k s. To investigate the effect of sintering temperature and heating time, the experiment of sintering at 1473K for 0.6k s and 1473K for 3.6k s was conducted. Microstructures of composites are revealed by Scanning Electron Microscope (SEM, TOPCON SM-520, Japan). The powder morphology and sintered microstructure were observed by Electron Probe Micro-Analyzer (EPMA, JXA-8900, Japan). X-ray diffraction (XRD; D/max-2500/PC, Japan) analysis was carried out using Cu Kα radiation (λ = 1.54056 Å) at a scanning speed of 1° /min over the 2θ range of

30°-75°. A hydraulic servo strength tester (SHIMAZU, EHF-LV020K1-020) is used for the tensile test of composite materials. Tensile test conditions are based on ASTM test method E8M-11, crosshead speed 0.5 mm / min. Strain gauge F-02W-12T11W3 (strain limit 2%, manufactured by Minebea Co., Ltd.) for Young's modulus measurement. The shape of the test piece of the tensile tester is shown in Figure 3.3(b). The fracture surface of the test piece after the tensile test is observed using SEM.

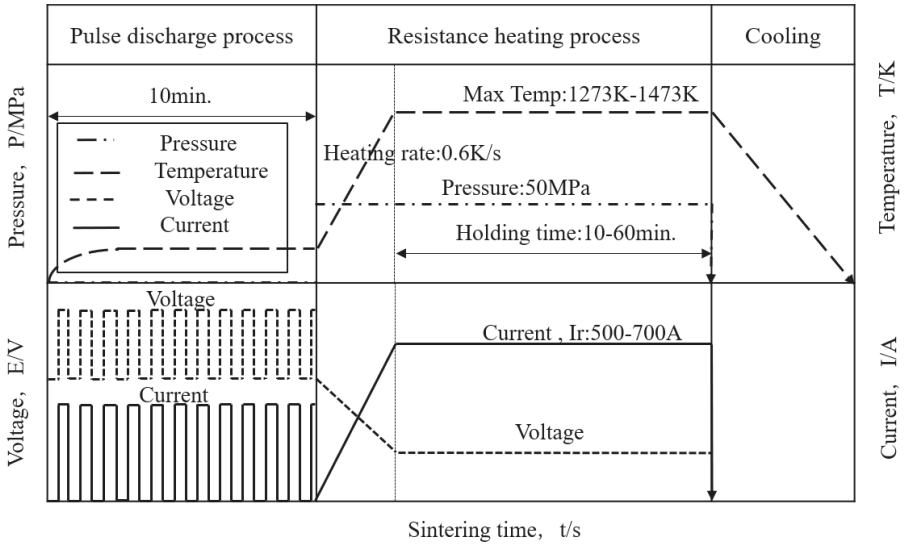

Fig. 3.2 Schematic illustration of processes of spark plasma sintering for large size.

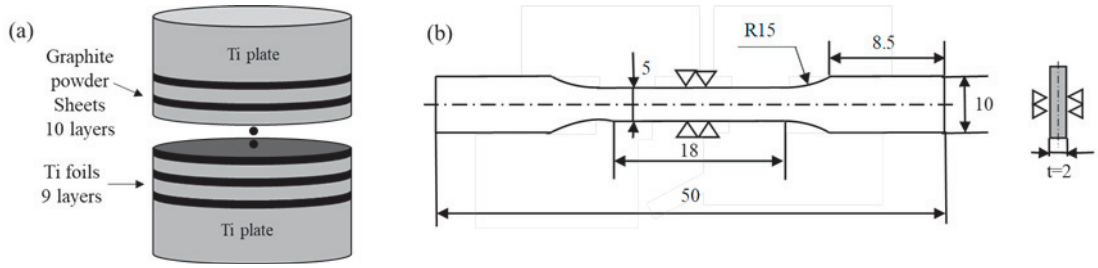

Figure 3.3. (a) Schematic illustrations of preparation processes of large-scale samples; (b) Image of shape of tensile specimen (ASTM test method E8M-11, unit: mm)

3.2.4 Hot forging of composite materials

We are currently trying to apply the composite material for golf clubs, which is manufactured by hot forging a titanium alloy bar into a predetermined shape. Therefore, hot forging is performed to evaluate the forgeability of the composite material produced. The manufacturing conditions for this composite material for hot forging are summarized in Table 3.1, and the schematic diagram is summarized in Fig. 3.4.

Table 3.1 Conditions of hot-forging.

Molding direction	Load (t)	Thickness (mm)	Temperature (℃)
Applanation	72	1.3 ~ 1.65	500

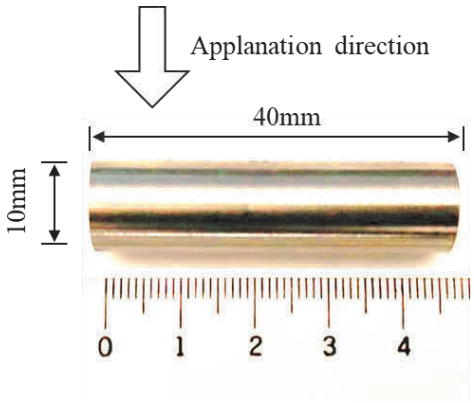

Fig.3.4 Schematic diagram of hot-forging composite applications in golf clubs.

3.3 Results and discussion

3.3.1 XRD

In order to investigate the mechanical properties of composites, large-scale multi-layered specimens of in-situ TiC reinforced TMCs were fabricated. Several layers of graphite powder sheets and titanium sheets were used as starting materials (as shown in Figure 3.2). Figure 3.5 shows XRD patterns of large-scale samples with different sintering temperature and heating time. It is evident from the Figure that each composite consists of TiCx and hexagonal close-packed (HCP) α-Ti. The sample with sintering temperature of 1473K for 3.6k s shows the biggest diffraction peak intensity.

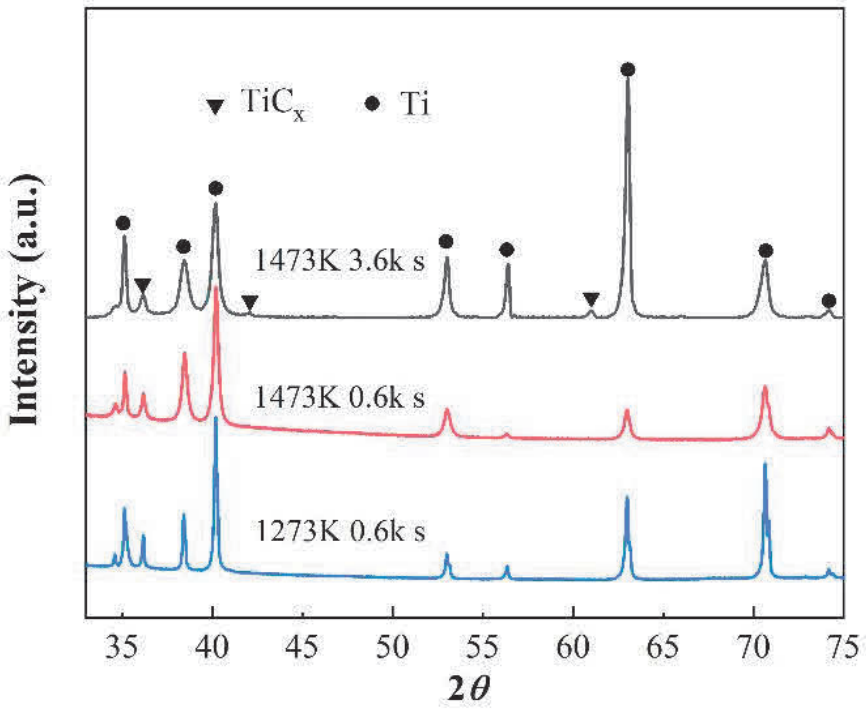

Figure 3.5. XRD pattern of TiC reinforced TMC sintered with different sintering temperature.

3.3.2 Microstructure

Figure 3.6 shows the microstructure of the large-size TiC reinforced TMCs. Figure 3.6(a) is the sintering temperature of 1273K for heating 0.6k s. For this sample, there are both dark lines and gray lines were observed. The dark line is considered to be residual graphite and the gray line is considered to be the TiC_x layer formed at the bonding area of Ti foils and graphite powder sheet. In Figure 3.6(b), by keeping the holding time constant for 0.6k s and increasing the sintering temperature to 1473K, there are no deep dark lines were observed instead a gray line appeared in the original position. It demonstrates the graphite has completely reacted with Ti matrix at 1473K. Figures 3.6 (c) and (d) are the samples of sintering temperature of 1473K for 3.6k s. In this sample, no obvious thick long lines were formed, instead numerous rod-like TiC_x particles were observed in the matrix and homogenous composite was obtained. In Figure 3.6(b), due to the short holding time, the C atoms in the graphite layer have not completely diffused into the Ti matrix, resulting in a locally high concentration of C atoms. Therefore, a layer-like TiC_x forms at the interface. When the holding time is increased to 3.6 ks, the sample is closer to thermodynamic equilibrium and most of the carbon atoms diffuse uniformly throughout the sample [14-15]. However, at the original position of graphite powder sheets, straight dotted lines formed by the arrangement of the short rod TiC can be still observed. The solid solubility of carbon atoms in titanium matrix is 0.05 wt% at room temperature, and 0.13 wt % above 1193K. Figure 3.6 (e) shows the schematic diagram of the ORs of TiC_x and α-Ti. The mechanism of formation of rod-like TiC_x particles were discussed in the following. Previous studies have already indicated the α-Ti co-deposited with TiC follows the crystallographic relationship: (0001) α // (111) TiC; [112(_)0] α-Ti // [110] TiC, in accordance with the TiC (111) preferred orientation. 8, [8, 16] As shown in Figure 3.6(c), the short rod-shaped TiC_x exhibits a regular angle to the direction of the Ti foils, at around 45 degrees. This is thought to be the carbon atoms precipitating out of the

titanium matrix and growing in a selective orientation along the (0001) α-Ti// (111) TiC. When the temperature is lower than 1155K, the atomic structure of titanium is HCP, and the solubility of carbon atoms in titanium is ~0.05 wt% [17]; when the temperature is higher than 1155K, the atomic structure of titanium is body-centered cubic (BCC), and the solubility of carbon atoms in titanium is ~0.15 wt%. When the temperature rises to 1153K, the C atoms are dissolved from the graphite powder sheets. Part of the C atoms diffuse into the Ti matrix. When the temperature falls below 1153 K, the C atoms precipitate due to the reduced solubility of the C atoms, and the precipitated C atoms diffuse into the titanium octahedral voids along the (0001) α-Ti// (111) TiC in a selective orientation, forming TiC_x. In addition, many TiC_x particles with an average diameter of about 1 μm can also be observed in Figure 3.6(c) and (d). TiC_x particles with two morphologies are present in the TMC prepared made from laminated stacks. Previous studies have demonstrated that the final shape of in situ TiCx is directly related to the value of x. [18] In C-atom vacancy structures, the number of C atoms is less than in structures without vacancies. Therefore, during the formation of TiCx crystals, the low C contributes to the atomic vacancies. As a result, it does not grow into a cube, but into a sphere. [18-21] Therefore, when the value of x turns low, the TiC particles do not grow into short rods, but into sphere particles.

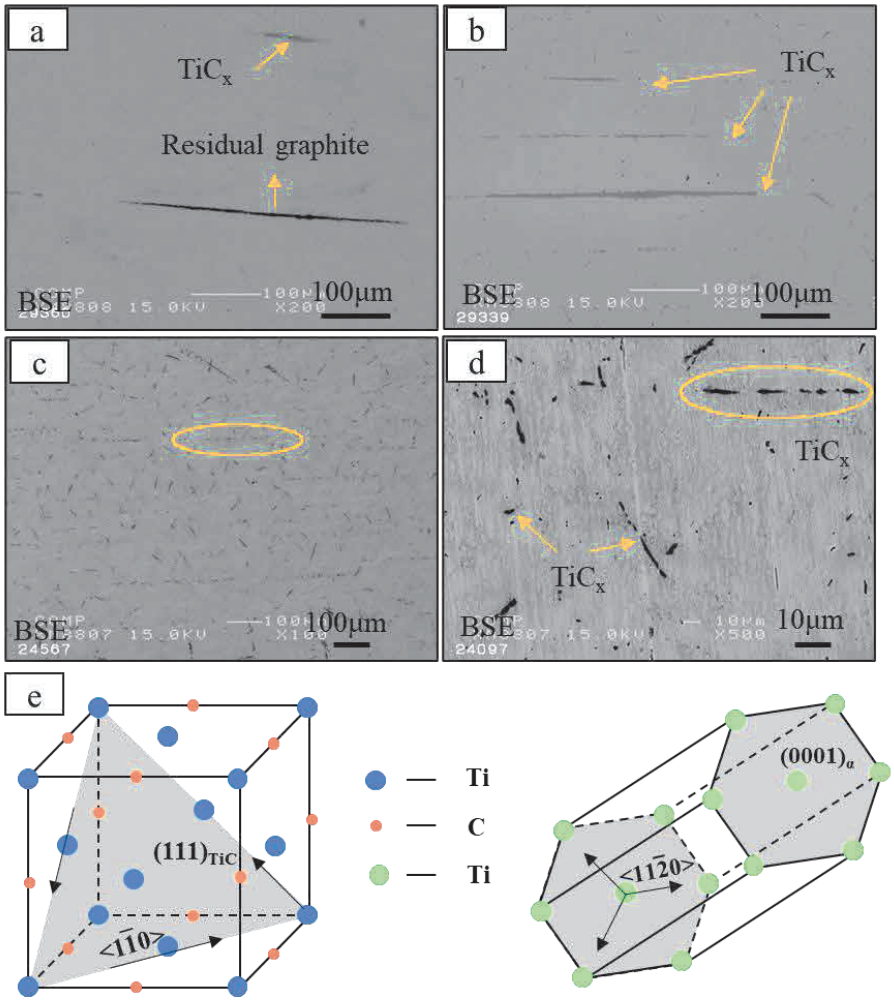

Figure 3.6. (a) BSE images of TiC reinforced TMCs sintering at 1273K for 0.6 ks; (b) 1473K for 0.6 ks; (c) and (d) 1473K for 3.6 ks; (e) The schematic diagram of the ORs of TiC and α-Ti.

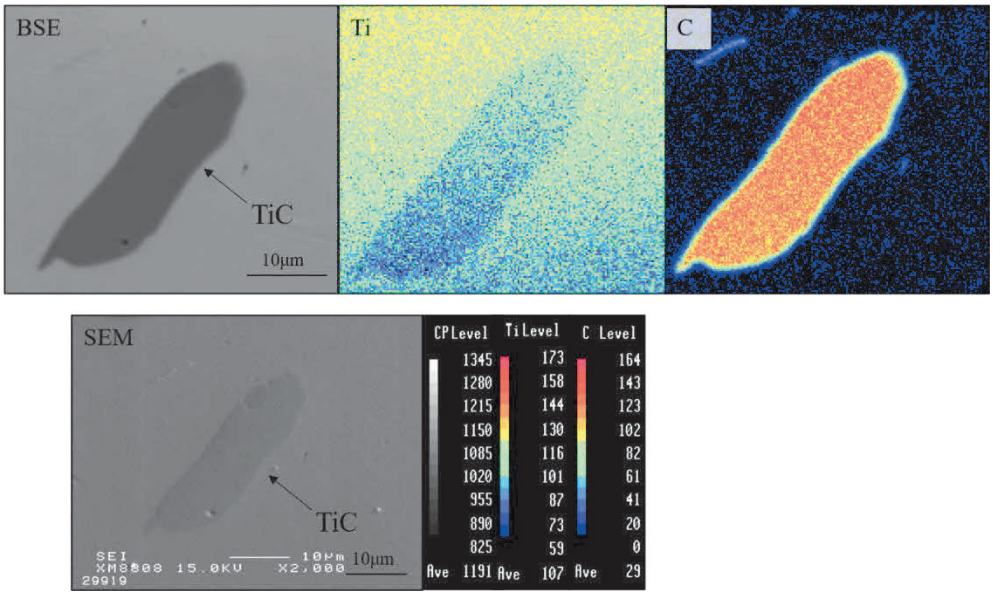

Fig. 3.7 Results of EPMA mapping and SEM image of TiC/Ti composite sintered at 1473K by SPS.

3.3.3 Tensile testing and strengthening mechanism analysis

Figure 3.8 shows the tensile stress-strain response curves for pure titanium and 1473 K TMC over 3.6 k s. The rod-like TiCx reinforcement improves the strength of the titanium matrix but reduces its ductility compared to pure titanium. The composites showed significant improvements with ultimate tensile strength (UTS) of 479 MPa, yield strength (YS) of 289 MPa and elastic modulus (E) of 234 GPa, 81.4 %, 140.8 % and 120.7 % higher than that of pure Ti, respectively. These enhancements came at the cost of ductility, which was reduced by 49.0%. Figure 3.9 shows the fracture diagram of the rod TiCx-reinforced TMC sample after tensile testing. As shown in Fig. 3.9(a), the composite shows typical ductile fracture characteristics with some river patterns and tear ridges clearly visible on the fracture surface. Some cracks can be observed in the corresponding magnified image of Figure 3.9(b). This observation suggests that the applied load may have been transferred from the substrate to the TiCx particles, since strong interfacial adhesion can provide effective load transfer capability and thus increase the yield strength [17]. Moreover, there are many ununiform dimples could be observed, which indicating good plasticity. Strengthening mechanism of rod-like TiCx particles in Ti matrx were discussed in the following. TiCx particles have excellent mechanical strength with an elastic modulus of 450 GPa, which is much higher than that of pure Ti (106.4 GPa). When load is applied to the composite, the hard TiC particles are able to bear part of the load. As shown in Figure 3.9(a), It shows a brittle fracture manner in the TiCx particles and ductile manner in the matrix. In addition, the in-situ synthesized TiCx particles have strong interfacial adhesion with the Ti matrix, which ensures an effective load transfer capability, thereby increasing the yield strength [16]. As shown in Figure3. 9(b), strong bonded interfaces between Ti and TiC transfer loads without debonding. In our work, the addition of a small amount of carbon (0.82 wt %) resulted in a significant increase in the tensile strength of the titanium matrix. However, the tensile properties of

our rod-like TiCx-reinforced TMCs are not outstanding when compared to the reference literature. For instance, Castro et al. [20] reported a 0.21 vol.% TiC-reinforced TMC by ingot casting metallurgy technique, with UTS of 565 MPa, which correspond to an increase of 47.4%, compared to pure Ti (UTS of 386 MPa). Lu et al. [21] reported a 3 wt.% PCS (polycarbosilane) of TiC-reinforced TMC by powder metallurgy, with UTS of 861 MPa, which correspond to an increase of 56.8%, compared to HDH (hydride-dehydride) pure Ti (UTS of 549 MPa). In contrast, although the UTS of our rod-like TiC reinforced TMC was 479 MPa, it significantly increased by 81.4% compared to the pure Ti (UTS of 264 MPa). As well known, the tensile properties of composites are also highly dependent on the matrix. Therefore, in future research, we will focus on improving the tensile properties of rod-like TiCx reinforced TMCs for example by changing matrix materials.

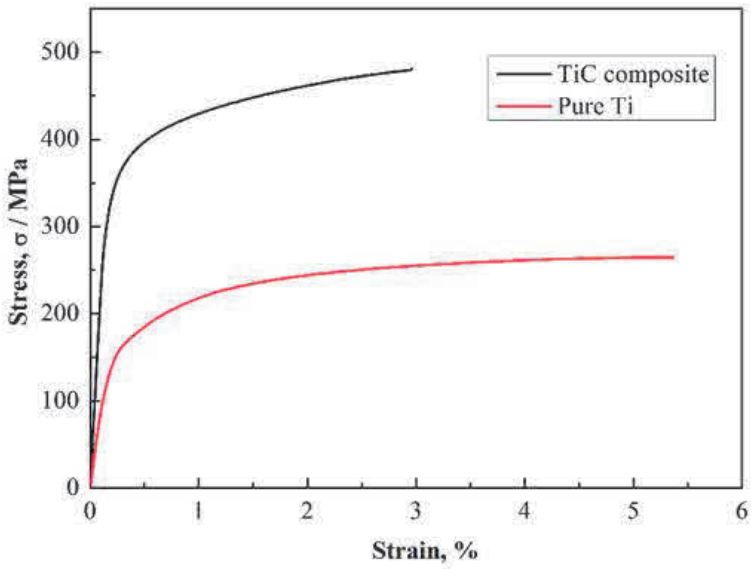

Figure 3.8. Tensile strength-displacement curve of of pure Ti and TiC reinforced TMC at 1473K for 3.6k s.

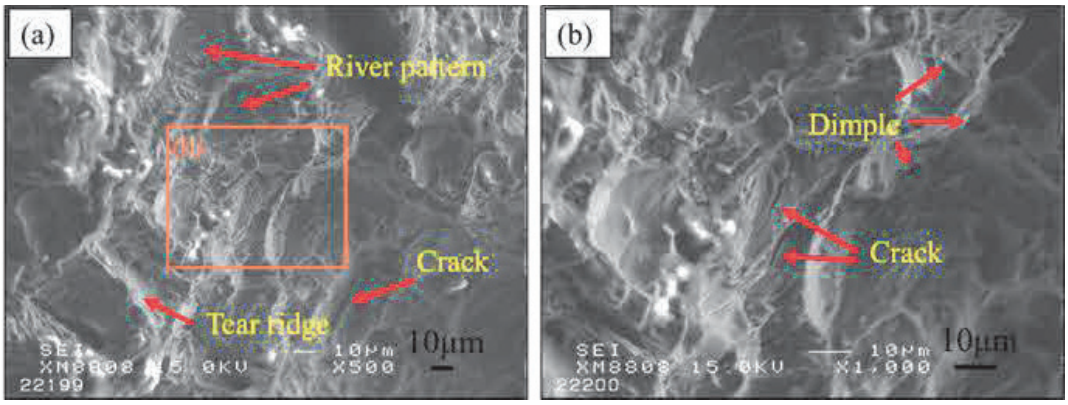

Figure 3.9. (a) SEM images of fracture surface of TiC reinforced TMC at 1473K for 3.6k s; (b) magnified image.

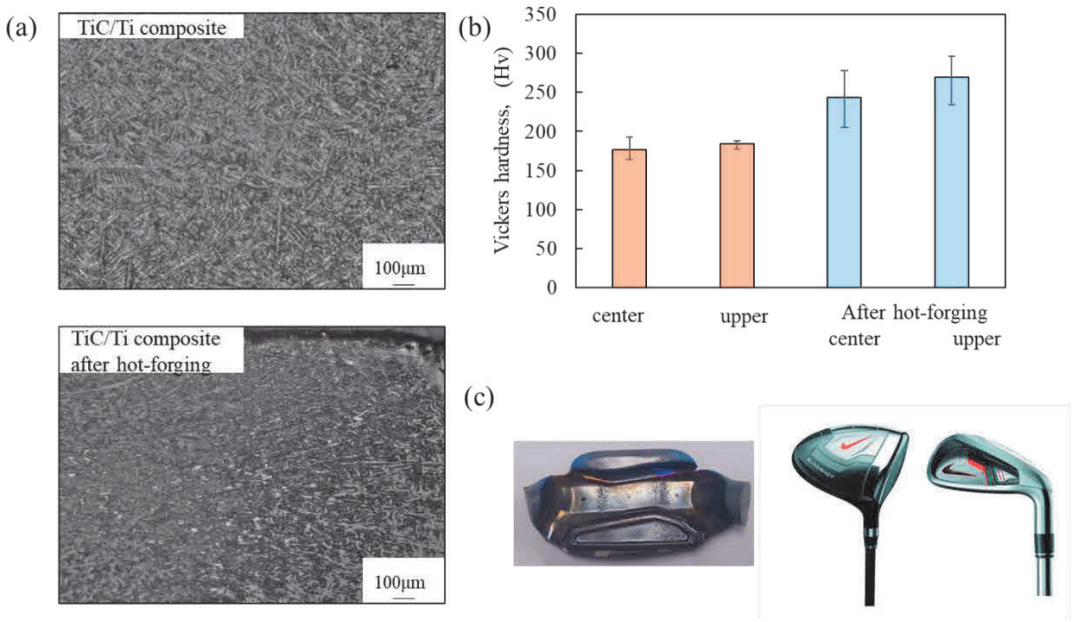

Fig.3.10 (a) OM images of TiC/Ti composite and TiC/Ti composite after hot-forging. (b) Measured values of micro vickers hardness test. (c) Application in golf clubs.

The composite structure after hot forging was etched and examined with an optical microscope, and the results were shown in Figure 3.10. For comparison, Figure 3.10 (a) shows the structure of the composite before and after hot forging. Before hot forging, the structure of the composite material is a comprehensive needle structure, and after hot forging, the structure of the composite material becomes a granular structure. This granular structure is often referred to as fiber flow. This structure can be observed by mirror-polishing and etching the metal. Fiber flow is a structure that forms when a metal is stressed, causing the crystals of the metal structure to collapse and become oriented, resulting in a linear flow. In general, impact values and fatigue limits show higher values when forces are applied along the fibre flow. The high durability resulting from this fiber flow is one of the characteristics of forged products.

In order to analyze the hardness difference caused by hot forging of composite materials made of molybdenum plates at 1473K freezing temperature, Vickers hardness tests were performed on the center and upper part of the two samples. A summary of the hardness test results is shown in Figure 3.10 (b). It is found that the hardness of the central part of the composite before hot forging is higher than that of the upper part. This is due to the high proportion of TiC and C particles in the center of the composite. After hot forging with molybdenum plate, the hardness of the central part of the sample increased by 53% compared with before forging, and the top part increased by 38%. This is because hot forging crushes the cavities inside the metal, making the crystal thinner and adjusting the crystal orientation. In addition, it can be seen from the standard error that the results of the upper part of the composite material vary greatly after hot forging. In this study, there are unreacted graphite powder sheets at the edge of the sintered composite. After hot forging, the unreacted graphite powder sheet exists around the composite substrate, which is believed to be the reason for the large changes in the upper part of the composite after hot forging.

Summary

(1) Graphite powder sheet and titanium plates were bonded together due to the solid phase reaction. TiC_x particles with an average diameter of 1μm were observed in the Ti matrix nearby the original position of graphite powder sheet.

(2) A homogenous rod-like TiC_x particles reinforced TMC using pure titanium foils and graphite powder sheet was fabricated by increasing the sintering temperature and holding time to 1473K for 3.6k s. XRD indicated all composites are composed of TiC_x and hexagonal close-packed (HCP) α-Ti.

(3) The rod-like TiC_x particles reinforced TMC have improved mechanical properties compared with pure titanium. The result of tensile test revealed the tensile strength of 479 MPa, yield strength of 289 MPa and elastic modulus of 234 GPa, which were 81.4 %, 140.8 % and 120.7 % increased, respectively.

References

[1] Tjong, S. C., Ma Z. Y.: Mater. Sci. Eng. R **29** (2000) 49-113.

[2] Hooyar A., Shima E. H., Damon K.:Mach. Tool. Manu. **133** (2018) 85-102.

[3] C. J. Zhang, F. T. Kong, S. L. Xiao: Mater. Sci. Eng. A **548** (2012) 152-160.

[4] Wang M. M., Lu W. J., Qin J. N.: Mater. Des. **27** (2006) 494-498.

[5] Ma F.C., Wang T. R., Liu P. Mater. Sci. Eng. **654** (2016) 352-358.

[6] M. F. Zawrah, M. H. Aly: Ceram. Int. **32** (2006) 21-28.

[7] W. H. Wei, Z. N. Shao, J. Shen: Mater. Sci. Tech-Lond (2017) 191-198.

[8] X.Y. Wang, S. P. Li, Y. F. Han: Compos. Part B Eng. (2022) 109511.

[9] L. Tsetseris, S. T. Pantelides.: Acta Mater. **12** (2008) 2864-2871.

[10] W. W. Sun, H. Ehteshami, Paul R. C.: Acta Mater. **15** (2019) 381-387.

[11] X.N. Mu, H.M. Zhang, H.N. Cai: Mater. Sci. Eng. A **687** (2017) 164-174.

[12] L.J. Huang, L. Geng, H.X. Peng: Mater. Sci. Eng. A **527** (2010) 6723-6727.

[13] Y.D. Tan, H.N. Cai, X.W. Cheng: Mater. Lett. **228** (2018) 1-4.

[14] J. Roger, B. Gardiola, J. Andrieux: J. Mater. Sci. **52** (2017) 4129–4141.

[15] J. Andrieux, B. Gardiola, O. Dezellus.:J. Mater. Sci. **53** (2018) 9533–9544.

[16] L. Y. Kuo, P.Y. Shen.: Mat. Sci. Eng. A **276** (2000) 99-107.

[17] X. Lu, Y. Pan, W.B. Li, M.D. Hayat: Mat. Sci. Eng. A **311** (2020)142-150.

[18] D.D. Zhang, H. L. Liu, L. P. Sun: Crystals **7** (2017) 205.

[19] D. S. Zhou, S. B. Jin, Y. J. Li : Cryst. Eng. Comm. **15** (2012) 643-649.

[20] V.de Castro, T. Leguey, M. A. Monge, A. Muñoz: J. Nucl. Mater. **31** (2002) 3127-3133.

[21] X. Lu, Y. Pan, W. B. Li: Mat. Sci. Eng. A **795** (2020) 139924.

Chapter 4

Effect of C content on the microstructure and properties of in-situ synthesized TiC particles reinforced Ti composites

4.1 Introduction 56

4.2 Experimental procedure 58

4.2.1 Preparation of graphite powder sheets 58

4.2.2 Fabrication of TiC/Ti composites 58

4.2.3 Characterization of TiC/Ti composites 59

4.3 Results and discussions 60

4.3.2 Microstructure characterization 61

4.3.3 Tensile testing 64

4.4 Discussion 67

4.4.1 Formation and Morphological Evolution of TiC 67

4.4.2 Strengthening mechanisms. 69

4.5 Summary 72

References 73

4.1 Introduction

Titanium matrix composites (TMCs) have received a lot of attention due to their application prospects in various industrial fields such as automotive, aerospace, biomedical, and military industries. These composites are known for their exceptional specific strength, excellent corrosion resistance and biocompatibility [1-6]. However, in today's rapid industrial development, traditional titanium alloys are difficult to meet the increasing demand for high-performance materials in rapid industrialization [3-7]. Titanium carbide (TiC), renowned for its high hardness, wear resistance, and corrosion resistance, is widely regarded as an ideal reinforcement material for ceramics due to its density and coefficient of thermal expansion closely resembling those of titanium and titanium alloys [7-9]. In situ synthesis of TiC reinforced TMCs involves exothermic chemical reactions with titanium groups through additives, which is considered to be one of the most promising processes because it not only improves the performance of the TiC reinforcement material and reduces the cost, but it combines the high strength of the reinforcement with the high plasticity of the titanium matrix [10-11]. The mechanical properties of TMCs mainly depend on the composition and microstructure of the matrix and particles. Ensuring the optimum strength and stiffness of these composites depends on precise control of the interface [12]. Previous studies have shown that uneven distribution of ceramic reinforcement in the metal matrix can lead to unsatisfactory mechanical properties[13]. Traditional composite preparation techniques, including powder metallurgy and combustion-assisted casting, often rely on powdered titanium as a raw material or necessitate extremely high temperatures to melt the matrix, significantly limiting large-scale composite production [13-14]. In consideration of energy consumption and sustainability, it is imperative to develop a cost-effective TMC preparation process that can further expand the application potential of these composites. Spark plasma sintering (SPS) is another technique suitable for the preparation of TMCs and has unique

advantages. However, there are currently limited data on the effects of SPS temperature on the microstructure and properties of graphite powder sheet and its related materials reinforced ti matrix composites. From the point of view of the formation of TiC in the heating process of titanium and carbon sources, SPS is an ideal choice for the preparation of Ti-TiC layered composites using titanium foils and different carbon sources [15-16]. It is known that sintering temperature and pressure have a significant effect on the densification behavior, microstructure evolution and property enhancement of matrix composites [17].

In this study, our primary objective is to ensure a comprehensive in-situ reaction and uniform distribution of reinforcement within Ti/C composites containing varying carbon contents. We prepared an ultra-thin graphite paper as the carbon source through a simple method, blending polyvinyl alcohol (PVA) and graphite powder, and controlled the carbon content by adjusting the amount of graphite powder. Utilizing 0.05 mm thick titanium foil as the titanium matrix, we employed a layer-stacking sintering method to fabricate TiC-reinforced TMCs. This approach avoided the use of powders and the high temperatures required for metal melting, thereby reducing costs. Additionally, the effects of carbon content on the morphology of the reinforcement, the evolution of the microstructure of the matrix and the mechanical properties of the composites were systematically investigated through composition design and process optimization.

4.2 Experimental procedure

4.2.1 Preparation of graphite powder sheets

Graphite powder sheets were prepared by mixing polyvinyl alcohol (PVA) powder as a binder and graphite powder in various ratios (3:1, 2:1, and 1:1) in a glass container containing deionized water (11.0 vol.% PVA solution). The mixture was stirred using a magnetic stirrer for 6 hours at 358K to achieve a homogeneous slurry, as depicted in Fig. 4.1 (a). This slurry was evenly applied to PTFE sheets and then placed in a drying oven at 338K for 12 hours to evaporate the solvent, resulting in the formation of graphite powder sheets. For comparison, pure PVA sheets were prepared using the same solution-evaporation method.

4.2.2 Fabrication of TiC/Ti composites

Commercial purity Ti foils (99.5%, thickness of 50 μm) and graphite powder sheets were cut into ϕ10 mm disks and then cleaned in an ultrasonic bath of ethanol for 20 minutes. The Ti foils and graphite powder sheets were alternately stacked and sintered in a vacuum SPS furnace, as shown schematically in Fig. 4.1 (b). For convenience, the fabricated composites with PVA sheets and graphite powder sheets were labeled as TMC-P, TMC-1, TMC-2, and TMC-3, corresponding to the content of graphite powder. It is noteworthy that PVA leaves carbon residues after high-temperature pyrolysis, following the removal of volatile gases. In this study, the PVA used had a 4% carbon residue after high-temperature pyrolysis under argon atmosphere, a result consistent with literature reports. Therefore, the actual carbon content includes the amount of added graphite powder and the carbon generated after pyrolyzing PVA. The carbon contents of the samples were calculated to be 0.18, 1.27, 1.81, and 3.91 wt.%, respectively.

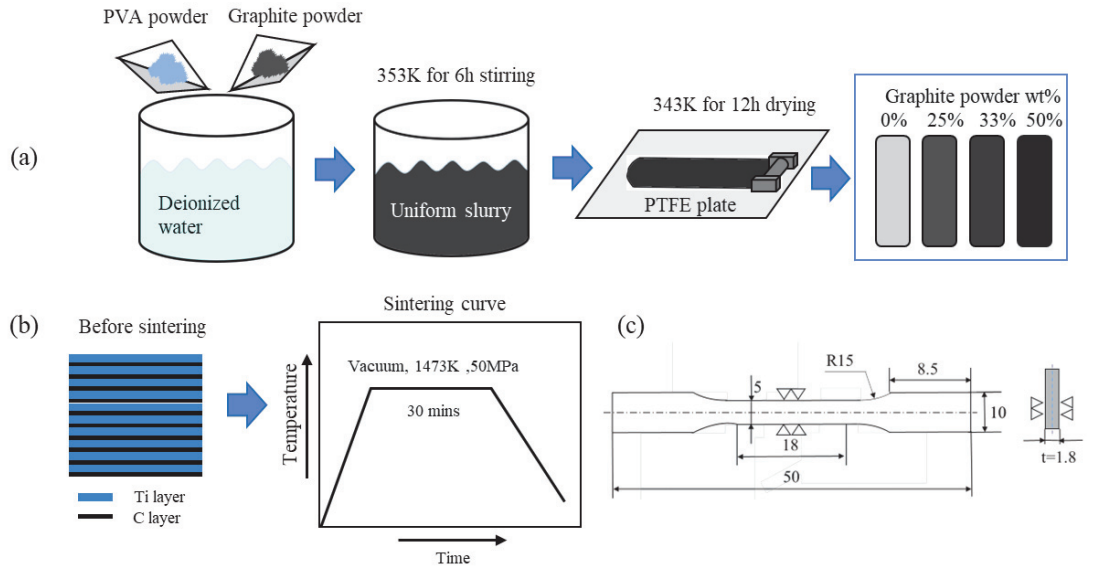

Fig. 4.1. (a) Schematic illustration of fabricating processes of graphite powder sheet; (b) sintering process of TiC/Ti composites; (c) size of plate tensile specimen.

4.2.3 Characterization of TiC/Ti composites

The fabricated composites were mechanically ground and polished perpendicular to the lamellas. Phase structures were characterized using an X-ray diffractometer (XRD, Rigaku, MiniFlex600) with Cu-Kα radiation. Microstructures were examined using a scanning electron microscope (SEM, JEOL, JXA-8900RL, Japan) equipped with a backscattered electron (BSE) detector. Semi-quantitative compositional analysis was conducted using energy-dispersive X-ray spectrometry (EDS) attached to the Zeiss microscope.

4.2.4 Mechanical Properties Measurement

Tensile strength and elongation percentage were determined for the samples using a Shimadzu AG-IS Tensile Tester and Trapezium-2 software in accordance with the ASTM test method E8M-11 standard, with a crosshead speed of 0.5 mm/min. The schematic illustration of specimen extraction and the dimensions of the tensile samples are depicted in Fig. 4.1 (c). Plate tensile specimens were polished before testing, and three specimens were tested for each set of measurements. Tensile fracture surfaces and subsurface morphologies were imaged using SEM.

4.3 Results and discussions

4.3.1 Phase characterization

Fig. 4.2 displays the X-ray diffraction (XRD) results of cross-sectional views of TiC/Ti composites with varying carbon contents. These results reveal that the composites consist of two phases: TiC and α-Ti. In the case of sample TMC-P, only the diffraction peak corresponding to the (200) crystal plane of TiC is observed, primarily due to its low carbon content. Comparing TMC-2 and TMC-3, a notable increase in the intensity of diffraction peaks is observed in the (220) and (311) planes with higher carbon content. This XRD analysis proves that TMCs reinforced with TiC can be fabricated by in situ technique utilizing the reaction between Ti and C.

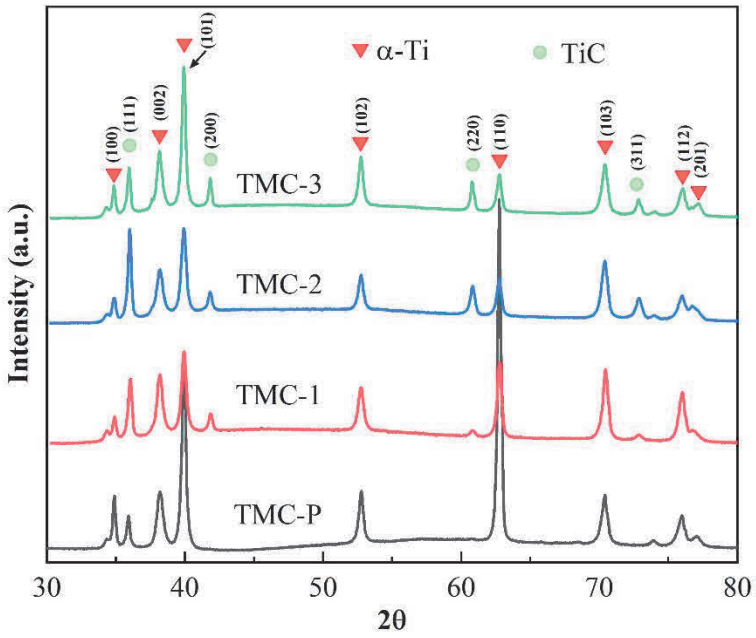

Fig. 4.2. X-ray diffraction pattern of deposited samples with different C content

4.3.2 Microstructure characterization

Fig. 4.3. illustrates the microstructures of sintered TiC/Ti composite materials with different carbon contents. It can be observed that all four composite materials prepared using the layer-stacking sintering method exhibit uniform microstructures. In samples TMC-P, as shown in Fig. 4.3(a), only a small number of gray particles and short rod-like eutectic TiC particles can be observed under magnification. From the high-magnification image, it can be observed that the particle size of the rod-like TiC is generally less than 5 μm. With an increase in carbon content to Fig. 4.3(b), the short rod-like titanium carbides disappear, replaced by discontinuous TiC layers appear at original graphite powder sheet positions within the composite. TiC exhibits a granular morphology with sizes mainly in the range from 5 μm to 10 μm, and at these discontinuous locations, two layers of titanium foils bonded together. When the carbon content increases to Figure 4.3(c), due to the increased thickness of the graphite powder sheet, the formed TiC particles are relatively larger and can be clearly observed. The composite material still maintains a uniform

distribution of TiC particles enhanced the morphology of the titanium matrix. Most of these TiC particles having diameters of around 10 μm. As the carbon content increases to Figure 4.3(d), a multi-layered structure of TMCs becomes apparent. However, it can also be observed that in some areas, the multi-layered structure of TiC exhibits discontinuous morphologies, possibly due to the non-uniformity of the original graphite powder sheets.

Fig. 4.4 presents high-magnification images of titanium carbide particles in the matrix, providing a detailed view of their morphology. Fig. 4 (a) shows the morphology of two rod-shaped TiC particles connected, with no discernible pores observed at high magnification. As the carbon content increases, the morphology of titanium carbide primarily exhibits a particulate form with different size, either existing independently or aggregated together, uniformly distributed at the interface of the two titanium layers. Moreover, noticeable pores are evident in the TiC layer, the quantity of which increases with the elevated carbon content. The formation of these pores may be attributed to the inefficient expulsion of gases generated during the decomposition of PVA at high temperatures. Alternatively, it could be due to residual carbon. If the cause is indeed residual carbon, increasing the insulation duration may assist in its removal. However, further investigation is necessary to pinpoint the specific cause.

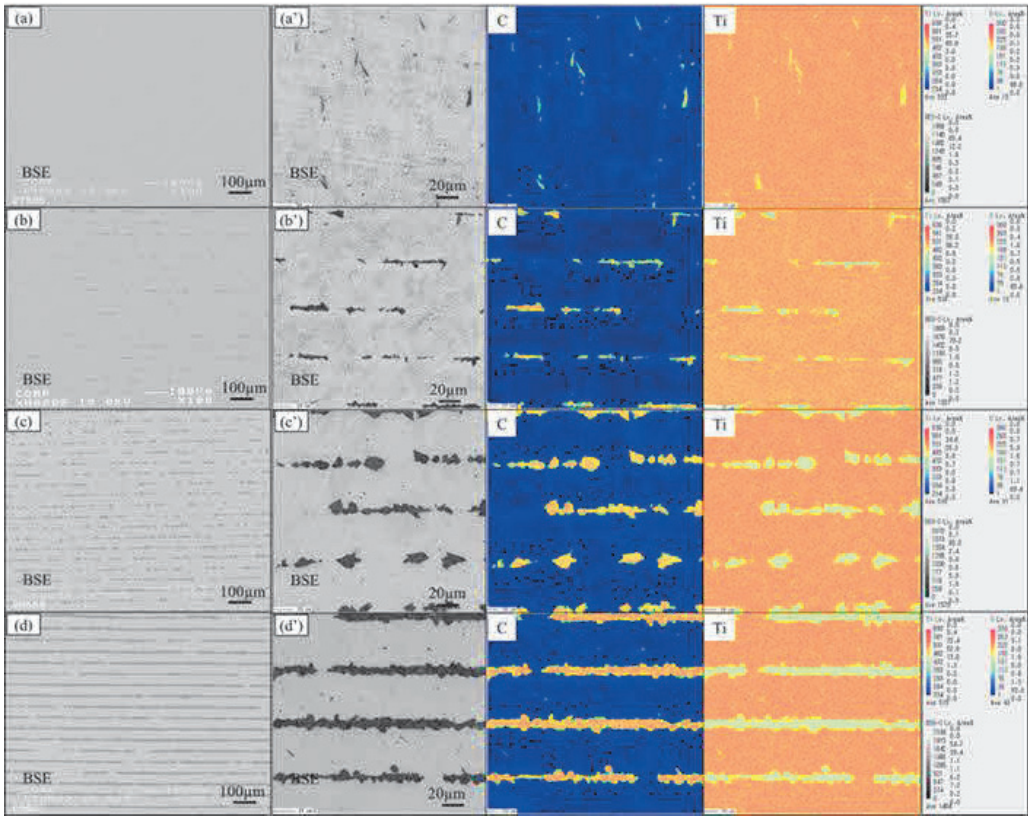

Fig. 4.3. Distributions of TiC particles inside of the TiC/Ti composites with different C content: (a) 0.18 wt.% of TMC-P; (b) 1.27 wt.% of TMC-1; (c) 1.81 wt.% of TMC-2; (d) 3.91 wt.% of TMC-3; (a') - (d') corresponding magnified mapping images.

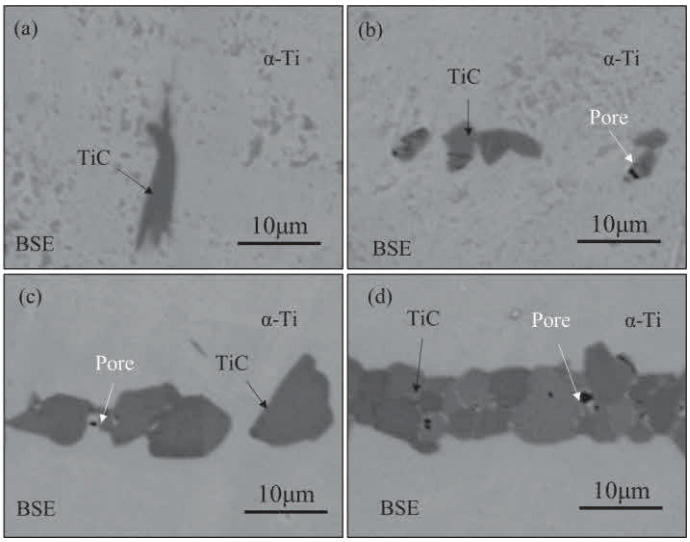

Fig. 4.4. High magnification BSE images of TiC/Ti composites with different C content: (a) 0.18 wt.% of TMC-P; (b) 1.27 wt.% of TMC-1; (c) 1.81 wt.% of TMC-2; (d) 3.91 wt.% of TMC-3.

4.3.3 Tensile testing

The room-temperature tensile results for TiC/Ti composites TMC-1, TMC-2, and TMC-3 are presented in Figure 4.4. It can be observed that the incorporation of carbon significantly enhances the performance of pure titanium in the TiC-reinforced titanium-based composites prepared through the layer stacking in-situ synthesis method. However, this improvement comes at the cost of reduced ductility in the composites. The yield strength (YS) and ultimate tensile strength (UTS) of pure titanium are 202.0 MPa and 348.7 MPa, respectively. When the C content increases to 1.27 wt% and 1.81 wt%, the UTS increases to 561.4 MPa and 575.4 MPa, showing improvements of 60.1% and 65.0% respectively, compared to pure titanium. However, the corresponding elongation decreases by 24.4% and 44.7%, respectively. When the C content rises to 3.9 wt%, the composites exhibit a multi-layered microstructure and the UTS of the composites reach 590.2 MPa. In comparison to composites with dispersed granular TiC microstructures,

there is no significant increase in tensile strength, but the elongation drastically drops to 3.26%, representing a decrease of 72.0%. The trend in the variation of tensile properties primarily arises from the lower C content, which results in smaller TiC particle diameters due to the thinner graphite powder sheet used. With an increase in C content, the diameter of TiC particles increases, and the particles exhibit distinct edges. Both of these samples share the morphology of discontinuous TiC particles uniformly distributed in the matrix. During tensile testing, the uniform dispersion of TiC particles significantly reduces the probability of localized stress concentration under external loading. This not only enables TiC particles to withstand higher stress during tensile testing but also reduces the rate of crack propagation. As the C content further increases, leading to a higher TiC content, the composite takes on a multi-layered structure. While the additional TiC particles enhance the strength of the composite, the clustering of TiC makes crack propagation within TiC more likely, leading to a drastic reduction in ductility.

Fig. 4.5 To further investigate the deformation behavior of the matrix, the loading effects of TiC, and the fracture mechanisms in the failed composite materials, the fracture surfaces of the failed composites were conducted. Comparing the fracture surfaces of TMC-1 and TMC-2, no significant changes were found except for more large depressions and more delamination in the TMC-2 matrix. No evidence of particle pull-out features was observed on the fracture surfaces of all three samples, indicating a good interfacial system between the TiC particles and the matrix. Many dimples were observed on the fracture surface of the Ti layers, indicative of ductile fracture. The TiC layer between the two Ti layers exhibited delamination and cracks, attributed to the mismatch in strain between TiC and the matrix. This observation suggests that the applied load have transferred from the matrix to the TiC particles, facilitated by strong interfacial adhesion that provided effective load transfer, thereby enhancing the yield strength [8]. Additionally, some bridging was observed. As for TMC-3, more extensive delamination and continuous bridging were evident, indicating that TiC particles significantly embrittled the matrix,

resulting in minimal plastic deformation. The bridging areas displayed crack surfaces, cleavage steps, and river patterns, signifying the coexistence of both brittle and ductile fractures.

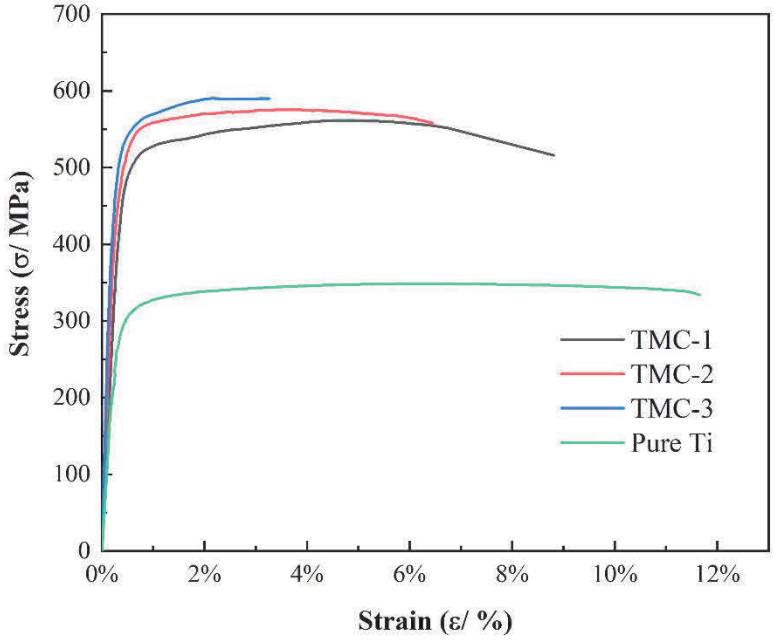

Fig. 4.5. Room temperature tensile stress-strain curve of deposited TiC/Ti composites.

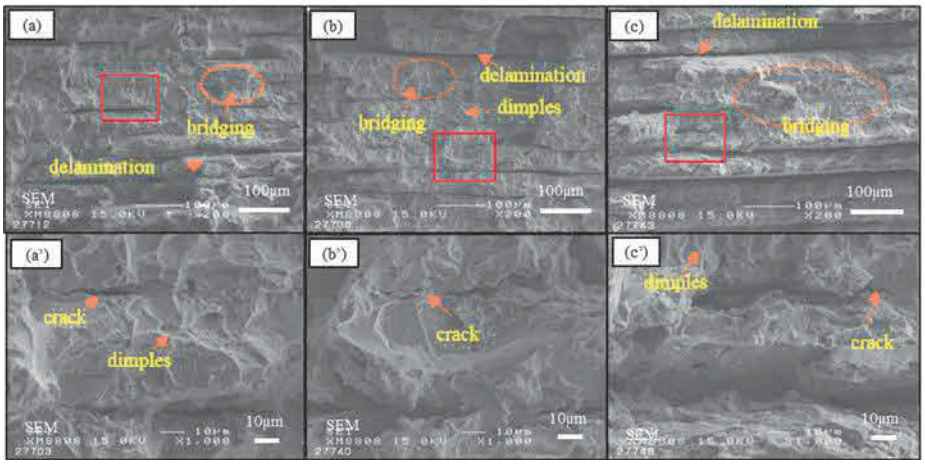

Fig. 4.6. Scanning electron micrographs of tensile fracture surface of the titanium matrix composites tested with different C content: (a) 1.27 wt% of TMC-1; (b) 1.81 wt% of TMC-2; (c) 3.91 wt% of TMC-3.

4.4 Discussion

4.4.1 Formation and Morphological Evolution of TiC

During the sintering process of composite materials, the principal mechanism responsible for the in-situ synthesis of TiC entails the diffusion of C atoms into the titanium matrix, leading to the subsequent formation of TiC. The feasibility of this reaction can be assessed through thermodynamic theory, which necessitates the computation of reaction formation enthalpy (ΔH) and Gibbs free energy (ΔG). As depicted below, under conditions where T < 1939K [18]:

$$\Delta H = -184571.8 + 5.042T - (2.425 \times 10^{-3} T^2) - (1.958 \times 10^6/T) \quad (4.1)$$

$$\Delta G = -184571.8 + 41.382T - 5.042T\, lnT + 2.425 \times 10^{-3} T^2 - 9.79 \times 10^5/T \quad (4.2)$$

Calculated results reveal ΔH = –183.7 KJ/mol and ΔG = –173.2 KJ/mol. The Gibbs free energy of the reaction is negative at a temperature of 1473K, indicating that the reaction can proceed spontaneously in thermodynamic range. Additionally, the formation enthalpy is also negative, representing the driving force behind the exothermic, self-sustaining, and rapid formation process of TiC.

TiC is a type of transition metal carbide distinguished by a face-centered cubic (FCC) NaCl-type structure, formed as smaller C atoms occupy octahedral positions, thus incorporating themselves into the titanium atomic lattice. Its actual composition typically deviates from stoichiometry and is symbolized as TiCx, where x signifies the ratio of C to Ti, with a range extending from 0.46 to 1.0 [18-20]. Below 1153K, the crystal structure of titanium adopts a hexagonal close-packed (HCP) configuration, with carbon atoms exhibiting solubility in titanium of approximately 0.05 wt%. Conversely, at temperatures surpassing 1153K, titanium adopts a body-centered cubic (BCC) crystal structure, and

the solubility of carbon atoms in titanium increases to around 0.15 wt%. These variations in carbon content influence the precipitation trajectory of TiC during the solidification process, ultimately shaping the morphology of TiC. In the TMC-P specimen, with a carbon content of 0.18 wt%, which is very close to 0.15 wt%, as the temperature reaches 1153 K, carbon atoms dissolve from the graphite layers, with some carbon atoms diffusing into the titanium matrix. As the temperature decreases below 1153 K, the reduced solubility prompts carbon atoms to precipitate, selectively diffusing along the (0001) α-Ti// (111) TiC planes into the tetrahedral interstices, replacing Ti positions, ultimately resulting in the formation of equiaxed TiC particles in the form of short rods or equiaxed shapes [3, 21].

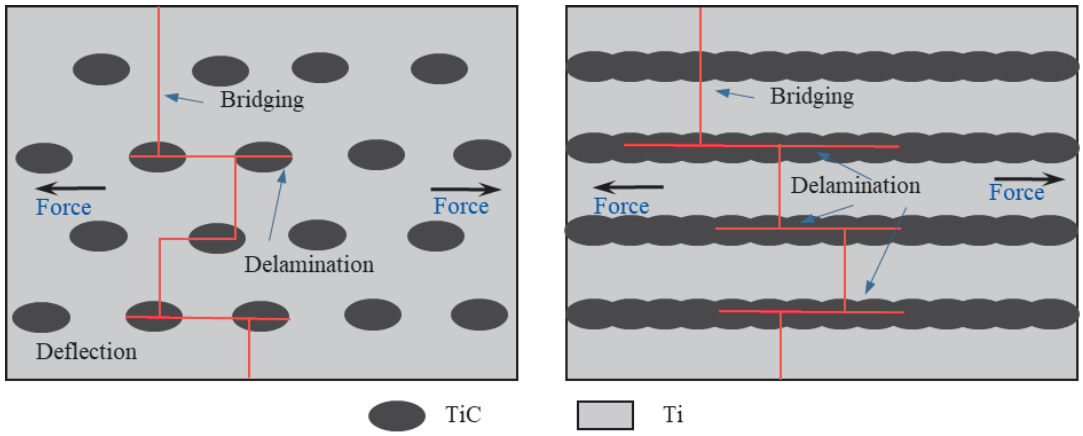

Fig. 4.6. Schematic shown crack propagation mechanisms for two types of structure.

4.4.2 Strengthening mechanisms.

TiC particles exhibit exceptional mechanical properties, with an elastic modulus of 450 GPa and a microhardness of 3200 kg/mm², significantly surpassing the mechanical performance of pure titanium (106.4 GPa and 150 kg/mm²) [8]. When the load was applied, the hard TiC particles can bare part of the load. Typically, the use of reinforcing materials to enhance the strength of TMCs is significantly influenced by the size, shape, proportion to the matrix, and the compatibility of the reinforcing material with the matrix. Additionally, the plastic deformation of the composite material is mainly affected by the matrix, and it is important to enhance the deformation resistance of the matrix, which is partly affected by the TiC content. For the strengthening factors of composite materials, it is generally believed that the strengthening effect of carbon mainly comes from two factors: one is the solid solution of C in the matrix, and the other is the bearing mechanism of TiC particles [22]. In the tensile tests conducted, the carbon content in all three samples exceeded the solubility limit in the titanium matrix. Furthermore, the increased matrix strength due to an elevated dislocation density constitutes a more pronounced strengthening effect.

Fig. 6 respectively illustrate schematics of the crack propagation mechanisms in discontinuous TiC particle-reinforced TMCs and multilayered TiC-reinforced TMCs. The crack propagation paths of the two structures are characterized by deflection and delamination, indicating that the ductile Ti layer can effectively release local stress and prevent crack propagation, thus improving the toughness of the composite. The Ti matrix between discontinuous TiC particles can accommodate more deformation, buffer the rapid expansion of cracks, and show better toughness. The fracture process of discontinuous TiC particle reinforced TMCs can be described by the fracture model proposed by Llorca and González. [23]At the initial stage of plastic deformation, with the matrix gradually strain hardening, the internal stress of the particles increases, resulting

in the fracture of the critical reinforced particles. The load released by the broken particles is mainly carried by the surrounding matrix. With increasing strain, the fractured particles disperse uniformly throughout the entire sample. However, when the matrix's strain-hardening capacity saturates, as the matrix can no longer harden, the stress released by the fractured particles is transferred to the neighboring particles. The stress acting on the adjacent particles increases, causing more particle fractures. The ultimate fracture of the composite material is attributed to the ductile failure of the matrix, based on nucleation and void growth [24].

As shown in Fig. 4.5, the fracture surface inspection confirmed the existence of TiC particle fracture, indicating that there is a strong interface adhesion between the in-situ synthesized TiC particles and the Ti matrix, thus ensuring the effective transfer of load and improving the yield strength. As the TiC particle fraction increases, the fracture surface becomes more uneven, resulting from the rapid extension of cracks. Notably, the particles in specimen TMC-2 are significantly larger than those in TMC-1. Once the TiC particle fraction is relatively high, especially with large particles and particle clusters in TiC, the cracks spread rapidly to the matrix due to the low plasticity of the matrix. Other studies have indicated that rapid coalescence of cracks occurs in large particles, leading to composite material fracture. Hence, reducing particle size may potentially improve the room-temperature tensile elongation of the composite material, which is worthy of further investigation. Furthermore, pores were observed on the surfaces of TiC in the discontinuous particle structure and in the composite materials with a multi-layered structure. These pores can also lead to premature failure. When microcracks form within the TiC crystals, they propagate along paths containing pores, accelerating the fracture of TiC crystals.

Additionally, an increase in the volume fraction of the reinforcement phase in multilayered TMCs results in an increase in dislocation density within the matrix, thereby improving yield stress. The fracture process in multilayered TMCs can be explained using

an equivalent strain model based on laminated theory during uniaxial tension tests [25]. Because the elastic modulus of Ti and TiC is different, the internal stress is different under the action of external force. With the increase of load, the Ti layer has plastic deformation, and the brittle TiC layer has micro-cracks and expands, releasing the internal stress. However, the ductile Ti layer prevents further crack propagation. With the increasing of tensile stress, in order to release the constraints around the ductile Ti layer, extensive plastic deformation occurs in the Ti layer. At this stage, the Ti layer starts to bear the load until it eventually fractures [26-27]. Larger particles and particle clusters are more prone to premature fracture due to greater constraints on plastic flow in the matrix, which has been supported by previous studies [22]. Within the particle clusters, triaxial stress is applied to cause fracture between particles and within the matrix. The matrix inside the particle cluster is fractured, which leads to the propagation of cracks inside the particle cluster, connecting adjacent particle clusters, and finally leading to macroscopic failure [24].

4.5 Summary

In this work, we prepared Ti-based composites with in-situ TiC reinforcement. Firstly, graphite powder sheets were prepared as carbon source and the pyrolysis product of PVA reacts with matrix Ti to form TiC. By adding graphite powder sheet with different C content and studying the influence of microstructure evolution and mechanical properties of composite materials, we draw the following conclusions:

(1) All composites are composed of only TiC and α-Ti and show uniform microstructure. When the carbon content is low, TiC presents approximately equiaxed rods; with the increase of C content, regular arrangement of discontinuous TiC particles reinforced TMCs were obtained. When the C content increased to 3.89wt%, a composite with multilayer microstructure was obtained.

(2) The mechanical properties of Ti-based composites are significantly improved. As the C content increases, the ductility of the composites decreases. Both TMC-1 and TMC-2 composites achieve a good combination of strength and ductility, with UTS of 561.4 and 575.4 MPa, YS of 275 and 354 MPa, and EL of 8.8% and 6.4%, respectively.

(3) The failure of all composites is triggered by TiC fracture. The discontinuous TiC structure can prevent the propagation of cracks, so that the composite can maintain good ductility, compared with the composite of multi-layer TiC structure.

References

[1] Liu D., Zhang S.Q., Li A. J. Alloy Compd. **485** (2009) 156-162.

[2] Hooyar A., Shima E. H., Damon K.: Mach. Tool. Manu. **133** (2018) 85-102.

[3] X.Y. Wang, S. P. Li, Y. F. Han: Compos. Part B Eng. (2022)109511.

[4] Lee W.H., Seong J.G., Yoon Y.H.: Cream. Int. **45** (2019) 8108-8114.

[5] Abkowitz, S., Abkowitz, S.M., Fisher, H.: JOM **56** (2004) 37-41.

[6] G.X. Li, K. Munir, C. Wen, Y.C J. Manuf. Process **56** (2020) 131-146.

[7] C. J. Zhang, F. T. Kong, S. L. Xiao: Mater. Sci. Eng. A **548** (2012)152-160.

[8] X. Lu, Y. Pan, W.B. Li, M.D. Hayat: Mat. Sci. Eng. A **311** (2020) 142-150.

[9] B.H. Li, Y. Liu, J. Li: J. Mater. Process. Tech. **210** (2010) 91-95.

[10] K. Vasanthakumar, S. Ghosh, N. Koundinya: Mater. Sci. Eng.A,**795** (2019) 30-39.

[11] S. Dadbakhsh, R. Mertens, L. Hao: Review. Adv. Energy Mater. **21**(2019) 1801244.

[12] F.C. Ma, J.J. Zhou, P. Liu W. Li: Mater. Charact. **127** (2017) 27-34.

[13] Liu Y.B., Liu Y., Tang H.P.: J. Alloy Compd. **509** (2011) 3592-3601.

[14] C.J. Han, R. Babicheva, J.D.Q. Chua: Additive Manufacturing, **36** (2010) 101466.

[15] Y.D. Tan, L.Y. Xu, Z.Q. Xu: Mater. Sci. Eng. A **767** (2019)138296.

[16] E. Ghasali, M.S. A. Nezhad S.: Ceram. Int. **45** (2019) 14045-14057.

[17] L.L. Dong, B. Xiao, Y. Liu: Ceram. Int.**44** (2018)17835-17844.

[18] W.H. Wei, Q. Zhang, W.J Wu: Scripta Mater.**187** (2020) 310-316.

[19] Y.X. Wang, H. Tan, Z. Feng: Mater. Sci. Eng.A,**855** (2022) 143935.

[20] L. Tsetseris, S. T. Pantelides: Acta Mater. **12** (2008) 2864-2871.

[21] W. W. Sun, H. Ehteshami, Paul R. C. Kent: Acta Mater. **15** (2019) 381-387.

[22] N. Wang, Y.B. Choi, K. Oue: Sci. Rep. **12** (2022) 19154.

[23] H.W. Wang, J.Q. Qi, C.M. Zou: Mater. Sci. Eng.A,**545** (2012) 209-213.

[24] J. Llorca, C. González : J. Mech. Phys. Solids, **46** (1998) 1-5.

[25] J.Q. Qi, H.W. Wang, C.M. Zou: Mater. Sci. Eng.A,**528** (2011) 7669-7673.

[26] Y.D. Tan, H.N. Cai, X.W. Cheng: Mater. Lett. **228** (2018) 1-4.

[27] Y.J Zhang, X.W. Cheng, H.N. Cai: Mater. Design, **92** (2016) 486-493.

Chapter 5

Conclusions

With the rapid development of electronic devices, traditional TMCs fail to meet the requirements of advanced electronics due to their low thermal conductivity and other inferior properties. While previous studies successfully developed advanced carbon TMCs with improved physical properties such as higher thermal conductivity, lightweight characteristics, and enhanced physical and mechanical stability compared to traditional TMCs, their properties have not been fully exploited due to complex manufacturing processes and high costs, making them challenging for practical applications. The objective of this thesis is to fabricate sheets using conductive fillers and PVA binder to achieve high thermal conductivity through a simple and cost-effective fabrication process. Additionally, an attempt is made to enhance the functionality of the sheets for practical applications. The conclusions of this thesis are summarized as follows:

(1) A manufacturing process has been developed for producing particle-reinforced titanium-based composite materials utilizing titanium plates and graphite powder sheets. The graphite powder sheet and titanium plates were bonded together through a solid-phase reaction occurring at temperatures exceeding 973K. It was observed that the bonding area increased with increasing temperature, reaching a bonding rate of up to 95% at a sintering temperature of 1273 K. Through surface analysis using EPMA and point analysis using FE-SEM, TiC particles with an average diameter of 1μm were identified within the Ti matrix near the original position of the graphite powder sheet. It was determined that the gray line observed at the junction of graphite powder sheets and the titanium matrix consisted of TiC and residual graphite.

(2) The graphite powder sheet and titanium plates were bonded together through a solid-phase reaction occurring at temperatures over 973K. It was observed that the bonding area increased with rising temperature. At a sintering temperature of 1273 K, the bonding rate reached up to 95%. TiCx particles with an average diameter of 1μm were observed within the Ti matrix near the original position of the graphite powder sheet. To fabricate large samples, a homogeneous rod-like TiCx particle-reinforced TMC was produced using pure titanium foils and graphite powder sheets by elevating the sintering temperature and prolonging the holding time to 1473K for 3.6k s. XRD analysis indicated that all composites were composed of TiCx and hexagonal close-packed α-Ti phases. The rod-like TiCx particle-reinforced TMC exhibited improved mechanical properties compared to pure titanium. Tensile testing results revealed a tensile strength of 479 MPa, yield strength of 289 MPa, and elastic modulus of 234 GPa, representing increases of 81.4%, 140.8%, and 120.7%, respectively.

(3) We fabricated Ti-based composites with in-situ TiC reinforcement. Initially, graphite powder sheets were prepared as the carbon source, and the pyrolysis product of PVA reacted with the matrix Ti to form TiC. By incorporating graphite powder sheets with varying carbon content and investigating their influence on the microstructure evolution and mechanical properties of the composite materials, it can be determined that all composites consist solely of TiC and α-Ti phases and exhibit a uniform microstructure. At low carbon content, TiC presents as approximately equiaxed rods; with increasing carbon content, TMCs with a regular arrangement of discontinuous TiC particles were obtained. When the carbon content reached 3.89wt%, a composite with a multilayer microstructure was achieved. The mechanical properties of Ti-based composites are significantly enhanced. As the carbon content increases, the ductility of the composites decreases. Both TMC-1 and TMC-2 composites demonstrate a good combination of strength and ductility, with ultimate tensile strengths (UTS) of 561.4 and 575.4 MPa, yield strengths (YS) of 275 and 354 MPa, and elongations at failure (EL) of 8.8% and 6.4%, respectively. The failure of all composites is triggered by TiC fracture. The

discontinuous TiC structure can prevent crack propagation, enabling the composite to maintain good ductility compared to the composite with a multilayer TiC structure.

Acknowledgements

I would like to dedicate my paper to all those who have offered me tremendous assistance.

First of all, my heartiest thanks flow to my supervisor, Associate Professor Choi, for his helpful guidance, valuable suggestions, and constant encouragement both in my study and in my life. His profound insight and accurateness about my paper taught me so much that they are engraved on my heart. He provided me with beneficial help and offered me precious comments during the whole process of my writing, without which the paper would not be what it is now.

Also, I would like to express my sincere gratitude to Professor Matsugi, who have taught me in this university that greatly broadened my horizon and enriched my knowledge in my study. His inspirational and conscientious teaching have provided me with a firm basis for the composing of this paper and will always be of great value to my future academic research. In addition, I would like to express my heartfelt thanks to Professor Sugio and Professor Sasaki for their technical advice and assistance to my doctoral thesis.

My thanks also go to the members of my lab whose monographs and academic ideas have enlightened me in my whole research life.

Finally, I would like to extend my deep gratefulness to my family and friends, especially my Xuan Chen, who encouragement and support have made my accomplishments possible.

Published papers in regard to this thesis

1. **N. Wang,** Y.B. Choi, K. Oue, K. Matsugi. Fabrication of in-situ rod-like TiC particles dispersed Ti matrix composite using graphite power sheet. Scientific reports. 2022(12) 19514. (Chapter 3)
2. **N. Wang,** Y.B. Choi, K. Matsugi. Effect of C content on the microstructure and properties of in-situ synthesized TiC particles reinforced Ti composites. Scientific reports. 2023(13) 22206. (Chapter 4)
3. Hot forging properties of TiC particles reinforced Ti matrix composite using graphite powder sheet, Yongbum Choi, **Ning Wang**, Kentaro Oue, Kazuhiro Matsugi, International Conference on Materials & Processing 2022 (ICM&P 2022)
4. Fabrication development of In-Situ TiC Particles Dispersed Ti Matrix Composite, **Wang Ning**, Yongbum Cho, Kazuhiro Matsugi, 2nd Japan-Korea collaborative Symposium in Advanced Composite Materials (2021)
5. Evaluation and Mechanical Properties of TiC Particles dispersed Ti Matrix Composite with graphite powder sheet, Kentaro Oue, Yongbum Choi, **Ning Wang**, Kazuhiro Matsugi and Xingang Liu, Asia-Pacific Conference on Fracture and Strength (APCFS2020)
6. **N. Wang**, Y.B. Choi, K. Oue, K. Matsugi, X.G. Liu. (2019). Fabrication of In-Situ TiC Particles Dispersed Ti Matrix Composite. International Conference on Precision Engineering and Sustainable Manufacturing（PRESM 2019）

Presentations

1. **N. Wang,** Y.B. Choi, K. Oue, K. Matsugi, X.G. Liu. (2019). Fabrication of In-Situ TiC Particles Dispersed Ti Matrix Composite. International Symposium on Precision Engineering and Sustainable Manufacturing. (PRESM 2019)
2. **N. Wang,** Y.B. Choi, K. Matsugi. G. Sasaki. (2023) Effect of carbon content on the microstructure and properties of in-situ TiC-Ti composites with graphite powder sheets as carbon source. (M&P2023)